Novel Genes Involved in Controlling Specification of *Drosophila* FMRFamide Neuropeptide Cells

Caroline Bivik, Shahrzad Bahrampour, Carina Ulvklo,[1] Patrik Nilsson,[2] Anna Angel,[3] Fredrik Fransson,[4] Erika Lundin,[5] Jakob Renhorn, and Stefan Thor[6]

Department of Clinical and Experimental Medicine, Linkoping University, Linkoping SE-585 85, Sweden

ABSTRACT The expression of neuropeptides is often extremely restricted in the nervous system, making them powerful markers for addressing cell specification . In the developing *Drosophila* ventral nerve cord, only six cells, the Ap4 neurons, of some 10,000 neurons, express the neuropeptide FMRFamide (FMRFa). Each Ap4/FMRFa neuron is the last-born cell generated by an identifiable and well-studied progenitor cell, neuroblast 5-6 (NB5-6T). The restricted expression of FMRFa and the wealth of information regarding its gene regulation and Ap4 neuron specification makes FMRFa a valuable readout for addressing many aspects of neural development, *i.e.*, spatial and temporal patterning cues, cell cycle control, cell specification, axon transport, and retrograde signaling. To this end, we have conducted a forward genetic screen utilizing an Ap4-specific *FMRFa-eGFP* transgenic reporter as our readout. A total of 9781 EMS-mutated chromosomes were screened for perturbations in *FMRFa-eGFP* expression, and 611 mutants were identified. Seventy-nine of the strongest mutants were mapped down to the affected gene by deficiency mapping or whole-genome sequencing. We isolated novel alleles for previously known FMRFa regulators, confirming the validity of the screen. In addition, we identified novel essential genes, including several with previously undefined functions in neural development. Our identification of genes affecting most major steps required for successful terminal differentiation of Ap4 neurons provides a comprehensive view of the genetic flow controlling the generation of highly unique neuronal cell types in the developing nervous system.

KEYWORDS *Drosophila*; CNS development; neural cell fate specification; forward genetic screening; FMRFamide

DURING nervous system development, a restricted number of progenitors generate the vast number of neurons and glia that build the mature central nervous system (CNS). The final identity of a specific neuron is dependent upon a complex series of regulatory steps, including spatial and temporal cues, asymmetric cell division, and terminal cell fate determinants (Allan and Thor 2015). In addition to the generation of a myriad of unique cell fates, each neural subtype furthermore is generated in precise numbers, and thus both proliferation and apoptosis are tightly regulated during development. In spite of tremendous progress during the last decades in deciphering these regulatory events, our understanding of how they integrate within the context of any specific neuronal lineage to ensure final cell specification and cell number is still fragmentary.

The *Drosophila melanogaster* CNS can be subdivided into the brain and the ventral nerve cord (VNC). The VNC is formed from the ventral part of the neuroectoderm by highly conserved anterior–posterior and dorsal–ventral patterning of the embryo (Skeath 1999; Skeath and Thor 2003). The VNC can be subdivided into three thoracic and 10 abdominal segments (Birkholz *et al.* 2013). During early embryogenesis 30 progenitors, denoted neuroblasts (NBs), are born in each hemi-segment (Bossing *et al.* 1996; Schmidt *et al.* 1997; Schmid *et al.* 1999). These undergo series of asymmetric divisions and produce distinct lineages of neurons and glia (Hartenstein and Wodarz 2013). Each NB has been assigned a name based on its row and columnar position and can be identified by its unique gene expression profile (Doe 1992; Broadus *et al.* 1995). One particularly accessible NB is the NB5-6, for which the entire lineage has been resolved in

doi: 10.1534/genetics.115.178483
Manuscript received May 21, 2015; accepted for publication June 16, 2015; published Early Online June 18, 2015.
Supporting information is available online at www.genetics.org/lookup/suppl/doi:10.1534/genetics.115.178483/-/DC1.
[1]Present address: Academedia AB, Stockholm SE-101 24, Sweden.
[2]Present address: E.ON Varme Sverige AB, Orebro SE-701 18, Sweden.
[3]Present address: Laboratoriet Vetlanda Vardcentral, Vetlanda SE-574 28, Sweden.
[4]Present address: SJ Gotalandstag AB, Nassjo SE-571 31, Sweden.
[5]Present address: Department of Immunology, Genetics and Pathology, Uppsala University, Uppsala SE-751 85, Sweden.
[6]Corresponding author: 3M-Lab1, Plan13, Campus HU, Linkoping University, Linkoping OG SE-58185, Sweden. E-mail: stefan.thor@liu.se

the thoracic and anterior abdominal segments (Schmidt *et al.* 1997; Schmid *et al.* 1999; Baumgardt *et al.* 2009; Karlsson *et al.* 2010). In the six thoracic hemi-segments, each NB5-6T generates a lineage of 23 cells, which can be readily identified by the expression of reporter genes under the control of an enhancer fragment from the *ladybird early* gene [*lbe(K)*] (Figure 1, A–C) (De Graeve *et al.* 2004; Baumgardt *et al.* 2007). The four last-born cells generated by NB5-6T express Apterous (Ap), a LIM-homeodomain transcription factor (Baumgardt *et al.* 2007). The very last-born is the Ap4 neuron that expresses the neuropeptide FMRFamide (FMRFa). After generation of the Ap4/FMRFa neuron, the NB exits the cell cycle and undergoes apoptosis (Baumgardt *et al.* 2009) (Figure 1C). The NB5-6T lineage displays an intriguing proliferation mode switch, wherein the neuroblast switches from producing intermediate progenitors (GMCs) into directly producing postmitotic neurons, and hence the Ap neurons are born directly from the neuroblast (Baumgardt *et al.* 2009; Ulvklo *et al.* 2012) (Figure 1C). This proliferation mode switch, called a type I $>$ 0 switch, from daughters dividing once to daughters that do not divide, was recently identified in many other developing lineages (Baumgardt *et al.* 2014). Failure to make this type I $>$ 0 switch results in the aberrant appearance of two Ap4/FMRFa neurons per thoracic hemi-segment (Ulvklo *et al.* 2012). In addition to these lineage properties of NB5-6T, previous studies have identified a number of regulatory cues and genes critical for generation of Ap4/FMRFa neurons. These include input from the temporal transcription factor cascade of *hunchback* $>$ *kruppel* $>$ *pdm* $>$ *castor* $>$ *grainy head*, which controls distinct competence windows in NBs (Brody and Odenwald 2000; Isshiki *et al.* 2001; Pearson and Doe 2004; Grosskortenhaus *et al.* 2005). Specifically, the late temporal genes *castor* (*cas*) and *grainy head* (*grh*) are critical for triggering proper expression of downstream determinants that dictate Ap4/FMRFa cell fate (Baumgardt *et al.* 2009). Furthermore, recent studies reveal critical upstream input also from the Hox homeotic system. The Ap neurons are produced only in the thoracic NB5-6 lineage, and recent work shows that the Hox gene *Antennapedia (Antp*), together with the Hox cofactors *homothorax* (*hth*) and *extradenticle* (*exd*), are critical for proper specification of the Ap4/FMRFa neurons (Karlsson *et al.* 2010). The upstream temporal and spatial cues result in the sequential activation of a distinct transcription factor code, which includes Ap itself, the basic helix-loop-helix transcription factor Dimmed (Dimm), the COE factor Collier (Col; FlyBase Knot), and the zinc-finger factor Squeeze (Sqz), as well as the Dachshound (Dac), Nab, Chip, and Eyes absent (Eya) transcriptional cofactors (Benveniste *et al.* 1998; van Meyel *et al.* 2000; Allan *et al.* 2003, 2005; Hewes *et al.* 2003; Marques *et al.* 2003; Miguel-Aliaga *et al.* 2004; Baumgardt *et al.* 2007, 2009). Finally, FMRFa expression is critically dependent upon a target-derived TGFβ/BMP retrograde signal, provided by the axonal target, the dorsal neurohemal organ (DNH) (Figure 1C). In the DNH, the BMP ligand Glass bottom boat (Gbb) activates the Wishful thinking (Wit) receptor, which activates the downstream effector phosphorylated Receptor-Smad protein Mad (pMad), which in turn enters the nucleus and acts synergistically with the intrinsic transcription factor code to activate FMRFa expression (Allan *et al.* 2003; Marques *et al.* 2003).

The invariant temporal appearance of one uniquely identifiable Ap4/FMRFa cell per thoracic hemi-segment, generated from an invariant and identifiable NB with a mapped lineage, combined with the existing insight into the regulatory cascades generating this neuron, makes FMRFa an excellent marker for assessing a wide range of developmental mechanisms. These include spatial establishment of NB identity, temporal progression in NBs, lineage progression and proliferation control, and cell fate specification. Moreover, the identification of *FMRFa* expression as being dependent upon target-derived TGFβ/BMP signaling fortuitously allows for utilizing its expression as a straightforward readout also of axon transport, axon pathfinding, and retrograde signaling. To pursue these issues in an unbiased and comprehensive manner, we have conducted a large-scale forward genetic screen based upon transgenic flies where the *FMRFa* enhancer drives enhanced GFP (eGFP) expression. This screen identified many of the known Ap neuron determinants, which validated the screen, but also a number of novel genes, presumably acting at various stages of NB5-6T development. All identified genes are lethal and have clear predicted human orthologs, but in spite of this, several have not been previously studied in the *Drosophila* CNS. These results provide an intriguing view of the genetic mechanisms underlying cell fate specification of a highly unique cell type in the CNS.

Materials and Methods

Fly stocks

The previously identified *FMRFa* Tv enhancer of 446 bp (Schneider *et al.* 1993) was amplified by PCR and inserted in the pGreenH-Pelican *P*-element vector (Barolo *et al.* 2000). Transgenic flies were generated by standard *P*-element transformation into w^{1118} flies. Initial *FMRFa-eGFP* transgenes eGFP at insufficient levels, and an X-chromosome insert was mobilized onto the autosomes by crossing to a *P* transposase source; *Delta2-3-99B* (BL#4368). A total of 120 novel autosomal *P*-element lines were analyzed, and one insert on each of the second and third chromosomes was identified, expressing sufficient eGFP levels for visual screening through the embryonic or larval cuticle. To facilitate for *P Gal4* recombination mapping, *UAS-myr-mRFP* (BL#7118 on the second and BL#7119 on the third) were first mobilized to generate more robust inserts and then recombined onto the *FMRFa-eGFP* chromosomes. However, this mapping approach was not pursued.

For validation of the reporter the following mutants were crossed into the transgenic reporter background: ap^{P44}, tup^{isl1}, *glass bottom boat* (gbb^{1}) (provided by K. Wharton),

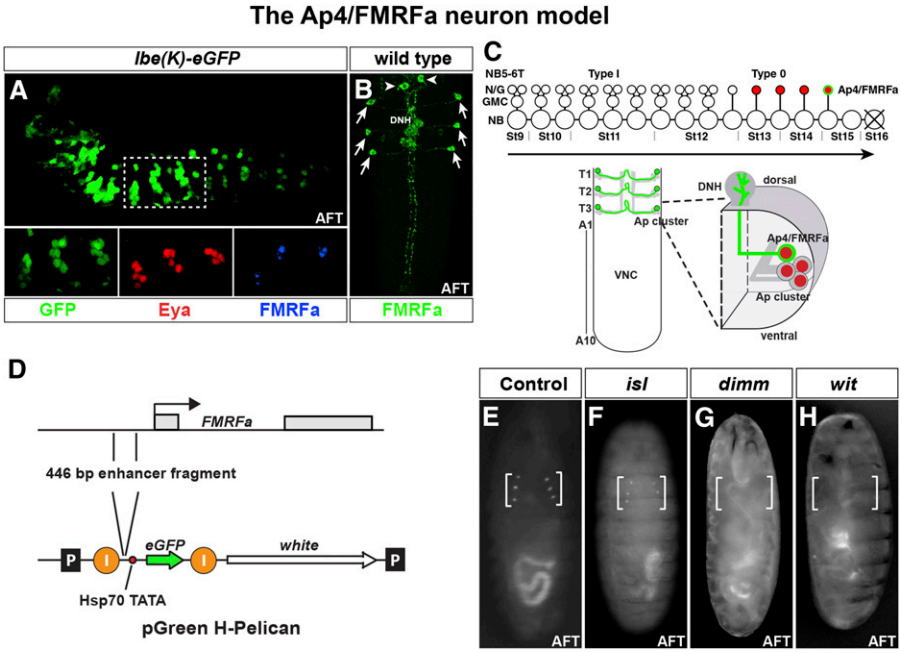

Figure 1 The lineage of thoracic neuroblast 5-6 and the Ap4/FMRFa neurons. (A) Expression of *lbe(K)-eGFP* reveals the NB5-6T lineage in the embryonic *Drosophila* VNC. In the three thoracic segments (T1–T3), the Ap clusters are generated at the end of the lineage and are identified here by Eya expression. The last-born cell, the Ap4/FMRFa neuron, is identified by FMRFa expression (lateral view, anterior left). (B) Expression of FMRFa in the developing *Drosophila* VNC stage AFT. FMRFa is expressed in the six Ap4/FMRFa cells in the three thoracic segments of the ventral nerve cord (arrows) and in the two SE2 cells (arrowheads) in the brain (dorsal view; anterior up). (C, top) Cartoon of the NB5-6T lineage progression. The early lineage is produced by nine rounds of type I divisions (NB > GMC > 2 postmitotic neurons/glia). At stage 12 there is a switch to type 0 division mode, and the five last neurons, including the Ap neurons, are born directly from the neuroblast. (C, bottom) The six Ap4/FMRFa neurons are depicted in the late embryonic VNC. Each Ap4/FMRFa neuron belongs to a group of four cells (five in T1), the Ap cluster, expressing the Ap gene. The Ap4/FMRFa neurons project axons to the midline and exit the VNC dorsally to innervate the DNH, where they receive critical input from the TGFb/BMP pathway. (D) Cartoon of the *FMRFa* gene and the *eGFP Drosophila* transformation vector pGreenH-Pelican. A 446-bp-long regulatory fragment that previously has been shown to drive FMRFa expression in Ap4/FMRFa neurons was cloned into the pGreenH-Pelican vector to drive eGFP expression. "I" denotes insulator sequences, and "P" the *P*-element 5′ and 3′ inverted repeats. (E–H) Live fluorescent microscopy images showing eGFP expression in *Drosophila* embryos at late embryonic stage with different genotypes to verify the validity of the reporter construct (ventral views). (E) In control, Ap4/FMRFa neurons are readily visible as six dots in late living embryos. (F) In *isl* mutants there is no effect on eGFP expression in the Ap4/FMRFa neurons compared to WT. (G and H) In *dimm* and *wit* mutants, there is a clear loss of eGFP expression.

$dimm^{P1}$ (provided by P. H. Taghert), wit^{B11}, tin^{346}, and $btn^{D3(3R)6273}$. For complementation analysis of mutants the following stocks were used: $dimm^{rev4}$ (provided by P. H. Taghert), $dimm^{P1}$, ap^{P44}, col^{1} (provided by A. Vincent), dac^{3}, gsb^{525}, mam^{8}, hth^{5E04}, nab^{R52} (provided by F. Diaz-Benjumea), sqz^{ie}, tin^{34b}, wit^{A12}, $cas^{\Delta 3}$ (provided by W. Odenwald), Mad^{10} (provided by I. Miguel-Aliaga), $mira^{L44}$ (provided by G. Technau), ago^{1} (provided by K. Moberg), Med^{1}, $zfh1^{00865}$, $ind^{16.2}$ (provided by R. Urbach), and *Df(lbl-lbe)B44* (provided by K. Jagla). Mutants where kept over *CyO, Dfd-YFP* (second chromosome) or *TM6b,Sb,Tb,Dfd-YFP* (third chromosome) balancer chromosomes. Unless otherwise stated, stocks were obtained from the Bloomington Drosophila Stock Center. The second and third chromosome deficiency kits were also obtained from the Bloomington Stock Center. Flies were raised at +26° on standard *Drosophila* medium. w^{1118} was used as wild type.

Mutagenesis

Batches of 50 *FMRFa-eGFP*, *UAS-myr-mRFP* males were treated together. Males were starved for 12 hr on water-soaked filter paper and then added to bottles containing filter paper soaked with 25 mM EMS and 1% sucrose in tap water. The flies were exposed for 12 hr and then allowed to recover on fresh media for 24 hr before mating en masse to *Sp, hs-hid/CyO,Dfd-YFP* or *hs-hid/TMB6B, Dfd-YFP* virgin females. Single F_1 male progeny were mated to 10 *Sp, hs-hid/CyO, Dfd-YFP* or *hs-hid/TMB6B, Dfd-YFP* virgin females for second or third chromosome balancing, respectively. After 5 days, the parents were discarded and the vials were heat-shocked at +37° for 40 min in a water bath to kill off all individuals carrying the *hs-hid* chromosome.

eGFP-based screen

Each balanced stock was first analyzed directly in the vial under a Leica fluorescent dissection microscope. Roughly one-third of lines generated viable mutant L1–L2 larvae, and because the eGFP signal was robust, the presence of the six Ap4/FMRFa neurons could be scored directly in the plastic vial. For lines that were embryonic lethal, embryonic collections were set up, and 10–15 late mutant embryos at the stage air-filled trachea (AFT) were observed as living whole-mount preparations under a Nikon Eclipse E600 FN Fluorescent Microscope with a FITC-HYQ filter. Affected lines from vial or whole-mount screening were classified according to eGFP expression and were subgrouped into five different classes: (1) no expression, (2) variable expression, (3) double cells, (4) ectopic expression, and (5) other phenotypes (Figure 4 and Figure 5).

PCR and sequencing of Sce^{08C065}

Homozygous mutant DNA was obtained from late embryos by scoring for the lack of *Dfd-GFP* (on the balancer chromosome). DNA was prepared using DNeasy Blood and Tissue Kit 5 (Qiagen, Hilden, Germany), according to the manufacturer's protocol. Primers covering a genomic 1474-bp segment,

including the two exons of *Sce*, were used to PCR-amplify the gene (forward primer: TTGGAAAATCTTAGCGAAAAT; reverse primer: AGAAATAAACGGCCTAATACTAAA). The PCR fragment was cloned into TOPO-TA Cloning (Invitrogen) and sequenced (GATC biotech, Konstanz, Germany), using M13 forward primer and M13 reverse primers.

Whole-genome sequencing

Nonallelic lines were crossed to each other, resulting in viable larvae (supporting information, Table S1). Genomic DNA was prepared from 20–30 wandering second or third instar larvae, using previously published methods (Blumenstiel *et al.* 2009). DNA was whole-genome-sequenced on the Illumina HiSequation 2000 platform (GATC Biotech, Constanz, Germany, or GeneWhiz, New Jersey, NJ) as unpaired 50- or 100-bp reads, and between 30–80 M reads per sample were achieved (Table S1) . Alignment of reads was performed using DNAStar 12, SeqMan NextGen software, and identification of mutations was performed using DNAStar, SeqManPro software (DNASTAR, Madison, WI). Due to the extensive mutagenesis caused by EMS treatment, multiple candidate genes were often identified, and an average of seven candidates were tested, first for lethality and second for eGFP phenotype.

Immunohistochemistry

Primary antibodies used for categorization of mutants were mouse mAb α-Eya 10H6 (1:250), mouse mAb α-Dac (1:25) (Developmental Studies Hybridoma bank, Iowa City, IA), mouse mAb α-Ubx (FP3.38; 1:10) (provided by R. White), guniea pig α-Dimm (1:1000), chicken α-proNplp1 (1:1000) and rabbit α-proFMRFa (1:1000) (Baumgardt *et al.* 2007), and rabbit α-pMad (1:5000) (provided by E. Laufer). Secondary antibodies used were FITC-conjugated donkey α-rabbit, rhodamine redX-conjugated donkey α-mouse, and Cy5-conjugated donkey α-guinea pig (1:200) (Jackson Immunoresearch Laboratories West Grove, PA). Immunostaining was conducted as previously described (Baumgardt *et al.* 2007). Preparations were scanned on confocal microscopes (Zeiss 700, Zeiss META, Zeiss Pascal). The Z-stacks were analyzed with the help of Zeiss LSM image software, and figures were assembled using Adobe Photoshop and Adobe Illustrator.

Results

Construction and validation of the FMRFa-eGFP reporter construct

The *FMRFa-eGFP* reporter was constructed by inserting a 446-bp-long fragment from the 5′ flanking DNA of the *FMRFa* gene into the pGreen H-Pelican vector (Barolo *et al.* 2000) (Figure 1D). The DNA fragment positioned 922–476 bp upstream of the first exon was previously shown to drive *lacZ* expression exclusively in the Ap4 neurons in late embryos and early larvae (Schneider *et al.* 1993; Benveniste *et al.* 1998). While the initial set of transgenes expressed specifically in Ap4 neurons, as detected by dissecting late embryonic and larval CNSs, none of them expressed at sufficiently high levels to allow for whole-mount eGFP detection in living embryos and larvae (not shown). To achieve high throughput in the screen we therefore mobilized an X-chromosome insert onto the autosomes and screened ∼120 new lines for eGFP expression. This resulted in the identification of two *FMRFa-eGFP* transgenic reporter strains, one on the second and one on the third chromosome, which consistently and reliably expressed eGFP at sufficiently high levels to be visible directly in living embryos and larvae (Figure 1E).

To facilitate for mapping of mutants using the genome-wide distribution of previously mapped *Gal4 P*-element inserts, a *UAS-myr-mRFP* transgene was recombined onto the *FMRFa-eGFP* chromosome on the second or third chromosome. However, this mapping approach was not subsequently used.

To determine if the *FMRFa-eGFP* reporter construct reliably reports perturbations of FMRFa expression, the reporter strains were combined with previously known genes that interfere with Ap neuron specification. As anticipated, embryos homozygous for mutations in the genes *ap*, *dimm*, *gbb*, *tin*, *wit*, and *btn* all showed <3% visible FMRFa/Ap4 cells compared to 91–94% visible FMRFa/Ap4 cells in the reporter strain control (Figure 1, E, G, and H; not shown for ap, tin, gbb, btn). In contrast, in embryos carrying mutations in the *isl* gene (FlyBase *tup*), which does not interfere with FMRFa expression, the eGFP signal was unaffected (data not shown) (Figure 1F). Taken together, these data show that the two *FMRFa-eGFP* strains predictably report on the effects of mutations in previously identified genes involved in the specification of the Ap4/FMRFa neurons and that the eGFP expression is robust enough to allow for a screen of living embryos and larvae.

Mutagenesis and screening of 9781 stocks identified 611 mutants

Homozygous isogenized *FMRFa-eGFP*, *UAS-myr-mRFP* males were treated with 25 mM EMS in 1% sucrose solution, using a standard protocol (Koundakjian *et al.* 2004). After recovery, mutated F_1 males were crossed with balanced females carrying a construct with the apoptosis-activating gene *hid* (Jiang *et al.* 1997) under the control of a heat-shock promoter. After 5 days, parent flies were discarded, and the vials were heat-shocked at +37° for 40 min. This led to death of all progeny carrying the *hs-hid* chromosome and left only the ones with correct genotype, *i.e.*, mutated *FMRFa-eGFP* chromosomes over *Dfd-YFP* marked balancer. By this procedure single mutated chromosomes were balanced and propagated in a high-throughput manner (Figure 2). Larvae and embryos homozygous for the mutated chromosome could be identified based upon *Dfd-YFP* expression from the balancer. The robust fluorescence from the *FMRFa-eGFP* reporter made it possible to screen roughly half of the mutants for aberrant phenotypes in living larvae. This was conducted by simply viewing larvae directly in the regular

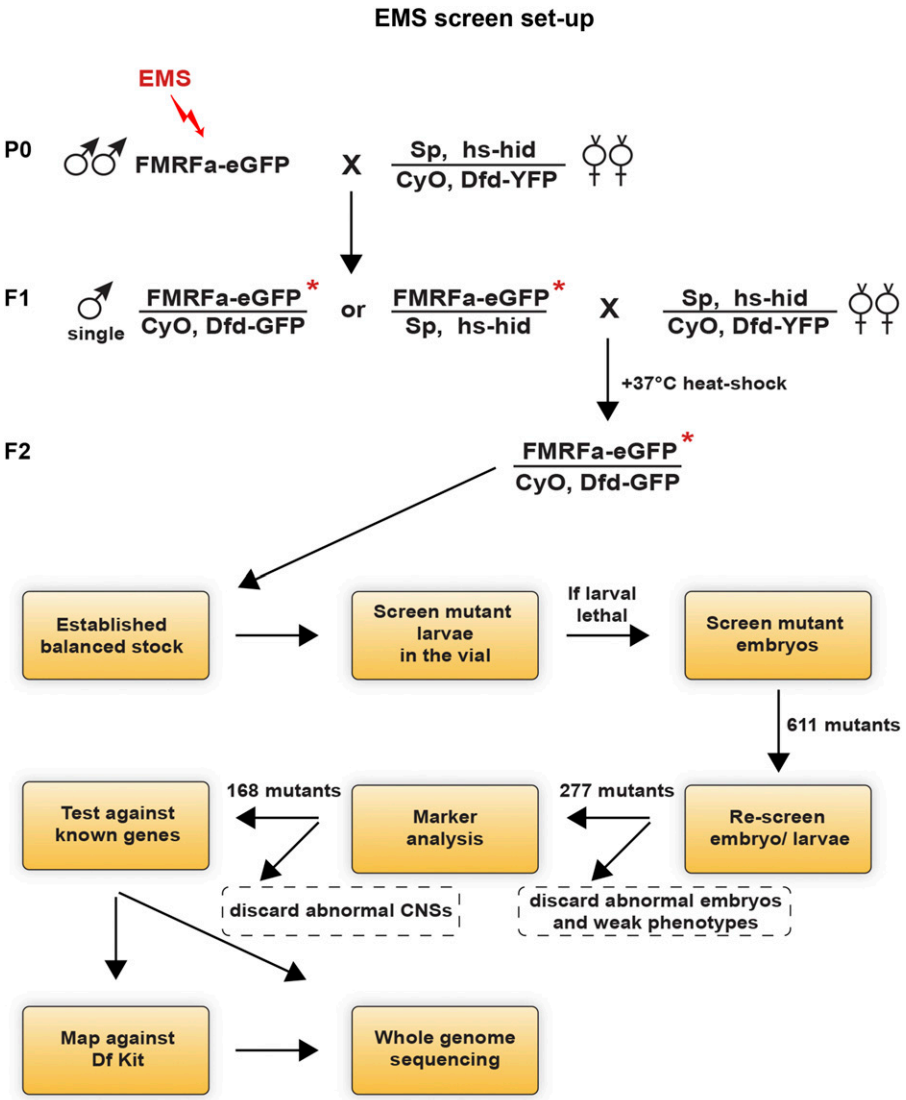

Figure 2 General outline of the fly crosses and the workflow used in the screen. Crosses are shown for the second chromosome. EMS-treated males were mated to *hs-hid* balancer virgin females, and F_1 single males from this cross were again mated to *hs-hid* balancer virgin females. Heat-shocking the progeny directly produced balanced stocks where each single mutated chromosome could be further propagated. Living embryos and larvae where thereafter screened for eGFP expressions under a fluorescence microscope. A similar crossing scheme was used for the third chromosome, using *hs-hid/TMB6B*, *Dfd-YFP*. Outlined below is the subsequent flow of the screen.

fly vial under a fluorescent dissection microscope (Figure 2). The other half, apparently larval lethal, were screened as late embryos. A total of 13 batches were mutated and 9781 balanced stocks were established, resulting in the identification of 611 mutants with altered *FMRFa-eGFP* expression.

Classification of mutants reveals numerous phenotypic categories

Mutants were initially categorized into different phenotypic classes based upon eGFP expression (Figure 3). The majority of mutants displayed absent, weak, or variable eGFP expression. A group (78 on the second and 37 on the third chromosome) displayed more global phenotypes, including malformed embryonic morphology and eGFP expression in tissues outside the CNS (Figure 3). However, a smaller number of mutants (24 on the second and 2 on the third chromosome) expressed eGFP in two or more cells in the same thoracic hemi-segment. Finally, another minor group (8 on the second and 3 on the third) displayed *FMRFa-eGFP* expression ectopically in other parts of the CNS. To validate the identified mutants, the 611 original mutants were rescreened, and 277 mutants with the strongest and most consistent eGFP phenotypes were selected for further analysis (Figure 2). For example, mutants that mostly showed loss of one of the six eGFP cells, and only loss of cells in some mutant embryos/larvae, were not pursued.

Previous work identified a multitude of markers expressed in Ap neurons (Benveniste *et al.* 1998; van Meyel *et al.* 2000; Allan *et al.* 2003, 2005; Hewes *et al.* 2003; Marques *et al.* 2003; Miguel-Aliaga *et al.* 2004; Baumgardt *et al.* 2007, 2009). By staining the 277 selected mutants with antibodies against these different identity markers, the GFP-based phenotypic groups could be further subdivided into different categories. To this end, mutants were immunolabeled against the transcription cofactor Eyes absent (Eya), which identifies the four Ap cluster neurons; the peptidergic transcription factor Dimmed (Dimm), which identifies the Ap4/FMRFa and the Ap1/Nplp1 neuropeptide cells; proFMRFa, for assaying endogenous FMRFa expression; and phosphorylated Mad (pMad), for TGFβ/BMP signaling specific to the

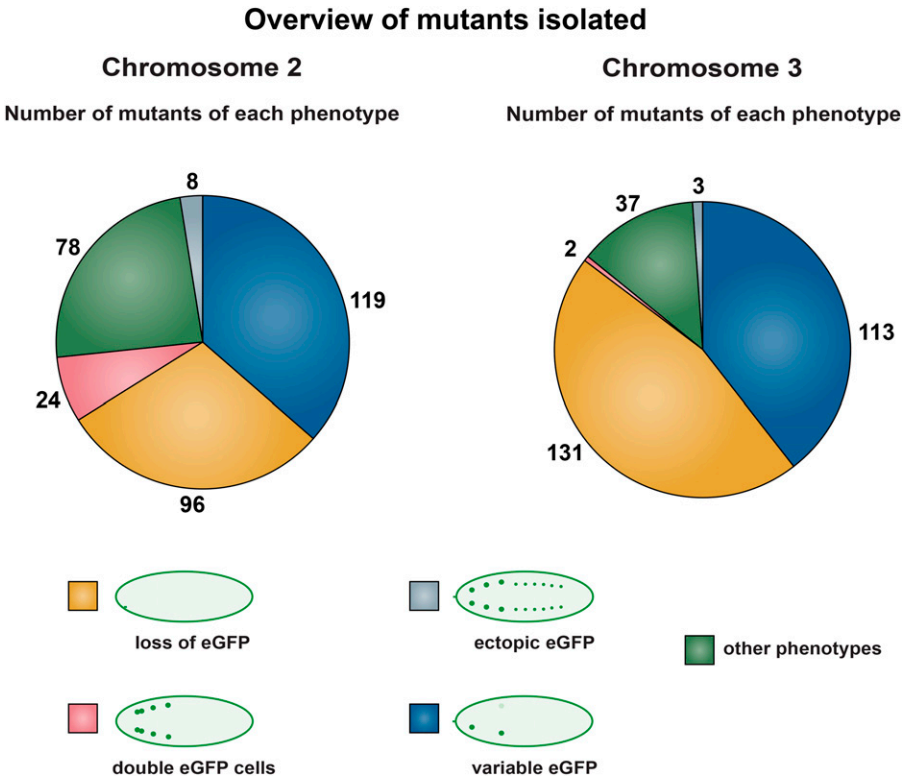

Figure 3 Overview of the five phenotypic categories identified. Phenotypic classes based upon *FMRFa-eGFP* expression among the identified mutants. From a total of 9781 mutant chromosomes, 325 and 286 mutants affecting *FMRFa-eGFP* expression were identified on the second and third chromosomes, respectively. The mutants were grouped into five categories based upon eGFP expression. The main part of the mutants showed none, weak, or variable eGFP expression. A small number of mutants (24 on the second chromosome and 2 on the third chromosome) instead expressed eGFP in an excess number of neurons. "Other phenotypes" refers to mutants with malformed embryos or other unspecific phenotypes.

Ap4/FMRFa neuron of the four Ap neurons (Figure 4, A, B, H, K, and N; Figure 5A; not shown for pMad in Ap4 neuron). This marker analysis discriminated several phenotypic categories (Figure 2). First, the staining for Eya could be subdivided into four groups: "Eya normal," "Eya missing," "ectopic Eya," and "Eya clumps" (Figure 4, C–G and H–P). The "Eya normal" group was subdivided by staining for Dimm, Nplp1, FMRFa, and pMad, which revealed subtype specification phenotypes of the Ap neurons. In the "Eya missing" group, two subgroups emerged: in one group Eya was missing globally in the entire VNC, while in the other, Eya was missing solely in the thoracic Ap clusters (Figure 4, C and D). One group displayed additional Eya expressing cells and contained two different subgroups; one in which ectopic Eya appeared in a regular striped pattern, while the second group displayed irregular "clumps" of Eya-expressing cells (Figure 4, E–G). The "ectopic Eya" group was analyzed regarding the downstream markers Dimm, Nplp1, and FMRFa. This revealed one group of mutants with an excess of Eya cells and ectopic Dimm expression but low levels of Nplp1 and FMRFa (Figure 4, E and F; only shown for Eya). Another group, on the other hand, had an excess expression of all four markers (not shown). Second, for assaying TGFβ/BMP signaling, accumulation of pMad was analyzed and two groups emerged; one group where pMad was affected globally (Figure 4P), and one group where pMad accumulation was affected only in the Ap clusters (Figure 4P; not shown).

This phenotypic subgrouping of alleles led us to candidate gene complementation tests against previously known mutants with similar marker effects. For example, mutants with global effects upon pMad staining were tested against the BMP/TGFβ pathway genes *Mad*, *gbb*, and *wit*. This resulted in the identification of several new alleles for *Mad* and *gbb* (Figure 4P; Table 1 and Table 2). Similarly, mutants with a complete loss of Eya were tested against Eya itself, as well as against important upstream regulators of Eya in the VNC, including *cas*, *col*, and *Antp*. This resulted in the identification of new alleles of *eya* itself, as well as of *cas*, *col*, and *Antp* (Figure 4, I, L, and O; Table 1 and Table 2).

Genetic mapping of mutants using the Bloomington Deficiency Kit

Our marker analysis of the 277 selected mutants revealed a number of mutants with grossly aberrant embryonic morphology or with disorganization of the CNS, as well as those with the "Eya clumps" phenotype. We envisioned that these mutants have disrupted genes primarily required for more general aspects of nervous system development, and not specifically associated with Ap4 neuron generation, and we do not describe these further here. For the majority of mutants, the initial marker analysis, and candidate complementation tests against known genes, failed to identify the affected gene. Thus, we initiated mapping of the mutants that displayed a morphologically normal CNS and did not map to previously known mutants by lethality mapping against a series of overlapping genomic deletions provided by the Bloomington Deficiency Kit: close to 200 stocks per chromosome. Mutants that failed to complement a certain deficiency, *i.e.*, that were lethal over the deficiency, were next tested against smaller deficiencies within the same

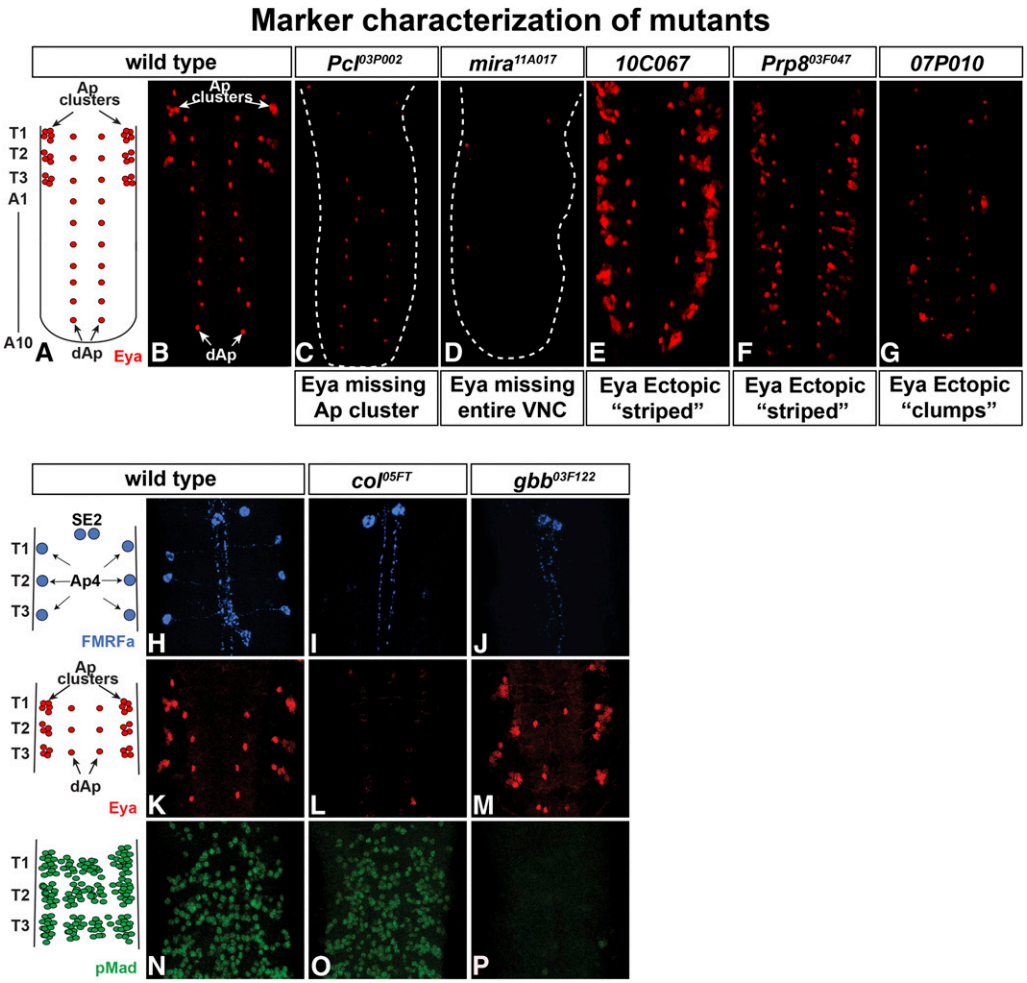

Figure 4 Aberrant Eya expression reveals different categories of mutants. (A and B) In wild type, Eya is expressed in the Ap cluster neurons in each thoracic hemi-segment, as well as in the two rows of dAp neurons. (C) One category of mutants, exemplified by *Pcl*^{03P002}, displayed loss of Eya expression in Ap clusters, but unaffected Eya expression in the dAp neurons. (D) Another category, exemplified by *mira*^{11A017}, displayed loss of Eya expression in the entire VNC. (E–G) Examples of mutants with additional Eya expression either in organized stripes (E and F) or in "clumps" (G). (H–P) Staining with antibodies to proFMRFa, Eya, and pMad further categorized mutants regarding Ap cluster specification and BMP/TGFb signaling. (H, K, and N) In wild type, FMRFa is expressed in the six Ap4/FMRFa cells in the ventral nerve cord and in the two SE2 cells the brain. Eya is expressed in the Ap neurons in each thoracic hemi-segment and in the dAp neurons. pMad is found throughout the VNC in motor neurons and susbsets of neuropeptide neurons, among them the Ap4/FMRFa neurons (Allan *et al.* 2003; Marques *et al.* 2003). (I, L, and O) The *col*^{05FT} mutant shows no endogenous FMRFa expression in Ap cells, while expression in SE2 cells is unaffected. Eya expression is lost in the entire VNC, while pMad staining is unaffected. (J, M, and P) In the *gbb*^{03F122} mutant, FMRFa expression is lost in the Ap4 neurons but maintained in the SE2 cells. Eya is expressed in both the Ap clusters and the dAp neurons, while pMad is lost from the entire VNC.

region and finally tested for lethality and phenocopy against candidate alleles within the smallest defined region. As expected from the typical regime of EMS treatment used in our screen, this revealed that many mutant chromosomes carried multiple lethal mutations when crossed to a deficiency, but not all displayed any eGFP phenotype. A total of 61 mutants were henceforth mapped down to 29 individual genes (Table 2). However, for some 45 mutants a shortage of alleles for many genes prevented mapping down to specific genes (not shown).

Mapping of mutants by whole-genome sequencing

Subsequent to the deficiency mapping, a subset of mutants (23) with a phenotype of interest, which had not been mapped by deficiency kit mapping, was mapped by whole-genome sequencing (WGS). This was conducted as previously described, *i.e.*, by crossing nonallelic mutants to each other and preparing DNA from L3 larvae (Blumenstiel *et al.* 2009; Gerhold *et al.* 2011). This use of nonallelic crosses ensured that viability, and thus L3 larvae, from which DNA can readily be prepared, were always recovered. The use of L3 larvae furthermore increased the amount of euchromatin DNA when compared to embryos or adult flies and hence increased the sequencing coverage of gene-dense regions. In addition, this provided multiple independent sequences of the starting chromosome, ensuring easy distinction between naturally occurring polymorphisms in the starting stock *vs.* mutations introduced by EMS mutagenesis. Each heterozygous sequence was aligned to the reference GenBank sequence and mutations observed in >29% of the reads were considered to be potentially caused by EMS. Nonsense or missense mutations in protein-coding genes were identified, and candidates were picked based upon gene expression (embryonic CNS) and/or known roles in development. An average of seven candidate genes per mutant was identified and tested by complementation to available alleles and/or a small deficiency spanning the gene. Nineteen of the 23 mutants analyzed by WGS were then mapped down to the gene (Table 2 and Table S1).

Spatial cues I: Polycomb group and Hox genes

The group of mutants lacking Eya expression specifically in the Ap clusters and not in dAp cells was identified as

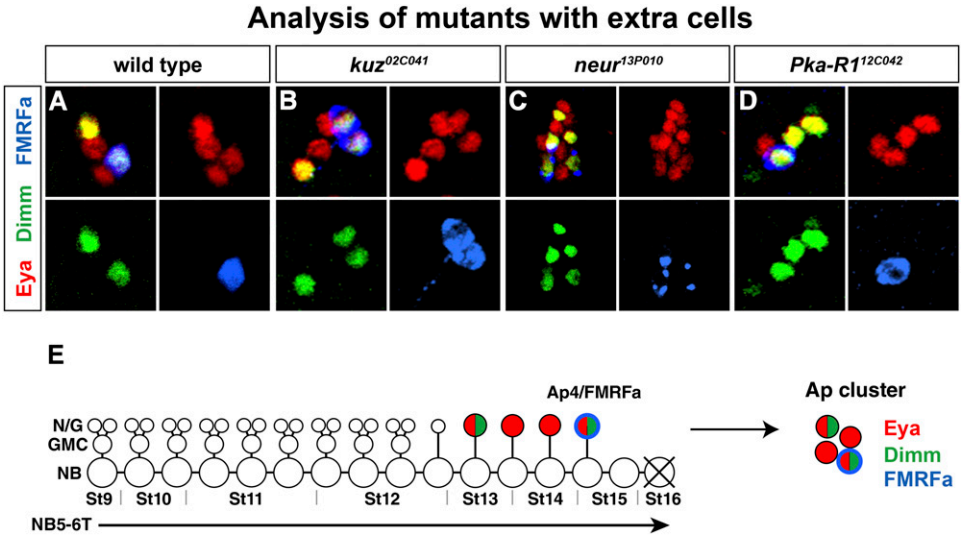

Figure 5 Expression of Ap cluster markers in wild type and in mutants with defects in Ap cluster composition. (A and E) In wild type, Eya identifies the four Ap cluster neurons and Dimm is expressed in the Ap4/FMRFa neurons and one additional peptidergic Ap cluster neuron, Ap1. (B) In *kuz*^{02C041}, Eya, Dimm, and FMRFa are expressed in an excess number of neurons. (C) In *neur*^{13P010}, Eya is expressed in up to 13 cells in each Ap cluster. Dimm and FMRFa are also ectopically expressed. (D) In *Pka-R1*^{12C042}, there is often one additional cell in the Ap cluster expressing Dimm.

belonging to the Polycomb group (PcG): *Polycomb* (*Pc*), *Polycomb like* (*Pcl*) (Figure 4C), *Sex combs extra* (*Sce*), *Sex combs on midleg* (*Scm*), and *Posterior sex combs* (*Psc*) (Table 2). *Scm*^{08C065} was further analyzed by PCR and DNA sequencing, and a nonsense mutation at amino acid 401 was identified (Table S1). Polycomb group proteins form large protein complexes known to repress the expression of Hox homeotic genes through histone modifications (Francis *et al.* 2001). Previous studies have demonstrated that Hox genes are critical for proper specification of the NB5-6 lineage. Specifically, *Antp* acts in concert with the temporal gene *castor* to activate key Ap neuron determinants in NB5-6T. In line with these roles of Hox genes during NB5-6T development, we also identified a novel allele of *Antp* in the screen (Table 2). In contrast, the Bithorax-Complex Hox genes acts in abdominal segments to ensure generation of the smaller NB5-6A lineage by an earlier cell cycle exit event (Karlsson *et al.* 2010). Because PcG is known to repress Hox gene expression, and limits the anterior extension of Hox gene expression, the identification of PcG genes in the screen likely reflects effects upon NB5-6T lineage development triggered by aberrant Hox expression. In line with this notion, we observe anterior expansion of expression of the Hox protein Ultrabithorax in *Sce*^{08C065} mutants (not shown).

Spatial cues II: columnar and segment polarity genes

In each developing VNC hemi-segment, a set of 30 identifiable and unique NBs are generated (Bossing *et al.* 1996; Schmidt *et al.* 1997; Schmid *et al.* 1999). The specification of NB identity is under the control of spatial information provided by the segment-polarity genes, acting to generate the seven distinct NB rows in each hemi-segment, and by columnar genes, which act to subdivide the neuroectoderm into three longitudinal domains (Skeath 1999; Skeath and Thor 2003). The combination of columnar and segment-polarity cues act in a Cartesian coordinate system to dictate NB identity (Skeath and Thor 2003). The homeodomain-encoding *intermediate nervous system defective* (*ind*) gene provides one of the columnar cues, being expressed in an intermediate stripe along the VNC and suppressing lateral NB identity (McDonald *et al.* 1998; von Ohlen and Doe 2000). We isolated an allele for *ind* in the screen, with a nonsense mutation at amino acid 279, and noted that it displayed extra Ap cluster neurons (Table 1, Table 2, and Table S1). Because NB5-6T is a lateral-most NB, and hence outside of the Ind expression domain, it is tempting to speculate that extra Ap neurons may indeed be ectopically generated by more medial NBs in *ind* mutants, but this idea remains to be tested.

Downstream of the segment-polarity and columnar cues, each NB identity is often driven further by additional regulators, although many of these are still unknown. With respect to row 5, several NBs in this row, including NB5-6, specifically express the related *ladybird late* (*lbl*) and *ladybird early* (*lbe*) homeodomain-encoding genes (De Graeve *et al.* 2004). Double mutants (overlapping deficiencies) displayed loss of lateral glia, generated in the early part of the NB5-6 lineage (De Graeve *et al.* 2004). We isolated an allele of *lbe* alone, with a nonsense mutation at amino acid 29, and found that it displayed loss of Ap cluster markers (Table 1, Table 2, and Table S1).

Temporal and NB identity genes

We isolated alleles for two temporal genes: *castor* (*cas*) and *grainy head* (*grh*), as well as for a temporal switching factor, *seven up* (*svp*) (Table 2). *cas* and *grh* are the last two transcription factors expressed in the canonical *hb* > *kr* > *pdm* > *cas* > *grh* temporal cascade. Both have been identified as important for the specification of Ap neurons, with a near-complete loss of FMRFa expression in each mutant (Baumgardt *et al.* 2009). *svp* is the *Drosophila* ortholog of COUP-TFI/II, an orphan member of the steroid/thyroid receptor superfamily (Pereira *et al.* 2000). *svp* was previously identified as being critical for proper down-regulation of Hb in the temporal cascade; however, this function does not in itself explain the phenotypes discovered in this screen. The identification of *svp* in the screen prompted us to recently investigate its function in greater detail, which revealed dual expression

Table 1 Summary of marker expression in the mutants mapped

Gene	GFP expression	FMRFa expression	Eya expression	pMad expression
kuz	double	double	extra	extra
neur	double	double	extra	extra
ind	double	double	extra	extra
seq	double	double	extra	extra
dap	double	double	extra	extra
brat	double	double	extra	extra
jhl-1	double	double	extra	extra
Surf6	double	double	extra	extra
svp	loss	loss	extra	loss
CG2469 (Ctr9)	loss	loss	extra	loss
grh	loss	loss	extra	loss
Prp8	loss	loss	extra	ND
cas	loss	loss	loss	loss
wor	loss	loss	loss	loss
kn (col)	loss	loss	loss	loss
eya	loss	loss	loss	loss
lbe	loss	loss	loss	loss
Antp	loss	loss	loss	loss
18w	loss	loss	loss	loss
Notum	loss	loss	loss	loss
Pc	loss	loss	loss	loss
Pcl	loss	loss	loss	loss
Psc	loss	loss	loss	loss
Scm	loss	loss	loss	loss
Sce	loss	loss	loss	loss
Rcc1 (Bj1)	loss	loss	loss	loss
CycE	loss	loss	loss	loss
CycT	loss	loss	loss	loss
E2f	loss	loss	loss	loss
mira	loss	loss	loss	loss
mute	loss	loss	loss	loss
mop	loss	loss	loss	loss
Cap-D2	loss	loss	loss	loss
glu	loss	loss	loss	loss
Nup358	loss	loss	loss	loss
sti	loss	loss	loss	loss
Pka-R1	loss/double	loss/double	normal	normal/extra
gbb	loss	loss	normal	loss
Mad	loss	loss	normal	loss
ago	loss	loss	loss/extra	loss
brm	loss	loss	normal	loss
pea	loss	loss	normal	loss
l(3)72Ab (Brr2)	loss	loss	normal	loss

Mutants were identified by FMRFa-GFP expression and subsequently stained for anti-proFMRFa, anti-Eya, and anti-pMad. This resulted in a subgrouping. As anticipated, all mutants with extra FMRFa-GFP expression also displayed additional proFMRFa, Eya, and pMad expression.

and function for *svp* in certain lineages, including the NB5-6T lineage (Benito-Sipos *et al.* 2011). The function of *svp* is complex, with mutants displaying loss of FMRFa but extra Ap cluster cells expressing Eya (Table 1), and is fully discussed elsewhere (Benito-Sipos *et al.* 2011).

We furthermore identified hits in two genes important for general NB identity and/or lineage progression: *worniou* (*wor*) and *sequoia* (*seq*) (Table 2). Wor is a member of the Snail family of zinc-finger transcription factors and plays important roles during early NB generation and development (Ashraf *et al.* 1999; Ashraf and Ip 2001; Cai *et al.* 2001). In line with this we observed loss of FMRFa and Ap cluster markers in *wor* (Table 1). Seq is a zinc-finger transcription factor highly related to *Drosophila* Tramtrack and was originally identified as causing extensive PNS sensory dendrite branching (Brenman *et al.* 2001). *seq* was subsequently re-isolated in a screen for bristle formation and found to control several regulators during bristle lineage development (Andrews *et al.* 2009). We noted extra FMRFa and Ap cluster markers in *seq*, indicating a role in cell specification and/or proliferation control (Table 1).

Chromatin modification factors

In addition to the PcG mutants identified, the screen revealed components of two other chromatin modification complexes. *brahma* (*brm*) is a component of the well-conserved SWI/SNF

Table 2 Summary of mutants mapped

Gene	Abbreviation	Gene ID	Predicted human ortholog(s)	Protein domains	Process	# of alleles	Alleles	Mapped by	Final complementation test against	Bloomington stock #
Polycomb	*Pc*	CG32443	*CBX8*	Chromo domain	Polycomb complex	1	*08P003*	Deletions	Pc^{1}	
Polycomblike	*Pcl*	CG5109	*MTF2*	Zinc finger, PHD, RING	Polycomb complex	4	*03P002, 04FG, 05F051, 05FAF, 07C098*	Deletions	Pcl^{11}	
Posterior sex combs	*Psc*	CG3886	*PCGF2*	Zing finger, PHD, RING	Polycomb complex	3	*03C041, 04P014, 04P022*	Deletions	Psc^{e24}	
Sex comb on midleg	*Scm*	CG9495	*SCML2*	Zinc finger, MYM-type	Polycomb complex	1	*12C011*	WGS	Scm^{D1}	
Sex combs extra	*Sce*	CG5595	*RNF2, RING1*	Zinc finger, RING-type	Polycomb complex	1	*08C065*	Deletions, PCR-seq	Sce^{1}	
Antennapedia	*Antp*	CG1028	*HOXA6*	Homeobox	DNA binding, Hox homeotic	2	*10C062, 12P003*	Deletions	$Antp^{12}$	
intermediate neuroblasts defective	*ind*	CG11551	*GSX1*	Homeodomain	CNS development, patterning	1	*10A013*	WGS	$ind^{16.2}$	59386
ladybird early	*lbe*	CG6545	*Lbx1*	Homeodomain	CNS, muscle and disc development	1	*12C005*	WGS	*Df(lbl-lbe)B44*	59385
seven up	*svp*	CG11502	*NR2B3*	Nuclear hormone receptor	Neuroblast temporal gene cascade	1	*11C115*	Deletions	svp^{1}	
castor	*cas*	CG2102	*CASZ1*	C2H2 Zinc finger	Neuroblast temporal gene cascade	4	*08A008, 08P007, 12P015, 13C011*	Deletions	$cas^{4\,3}$	
grainy head	*grh*	CG42311	*GRHL1*	CP2 transcription factor	Neuroblast temporal gene cascade	2	*05P010, 07C080*	Deletions	grh^{IM}	
worniu	*wor*	CG4158	*SNAI3*	Zinc finger	Neuroblast indentity	1	*04C042*	Deletions	wor^{1}	
sequoia	*seq*	CG32904	*PRDM10*	Zn finger, PR domain	Nervous system development	1	*03FH*	Deletions	$seq^{ve5\text{-}5}$	
CG2469	*CG2469*	CG2469	*Ctr9*	Tetratricopeptide TPR1	Paf1 Chromatin Complex	2	*09P004, 12P023*	Deletions	*Df(3L)BSC250*	59388, 59389
brahma	*brm*	CG5942	*SMARCA4*	Bromodomain	SWI/SNF component	1	*12C020*	Deletions	brm^{121}	
knot (collier)	*kn (col)*	CG10197	*EBF1/2/3/4*	bHLH	Transcription factor	3	*02F034, 03P091, 05FT*	Deletions	col^{1}	
eyes absent	*eya*	CG9554	*EYA1*	EYA domain	Transcription co-factor, phosphatase	2	*07P019, 07A002*	Deletions	$eya^{CII\text{-}IID}$	
glass bottom boat	*gbb*	CG5562	*BMP8A*	TGFb-related	BMP/TGFb ligand	2	*03F122, 04FK*	Deletions	gbb^{1}	
Mothers against dpp	*Mad*	CG12399	*Smad2*	SMAD domain	TGF beta signal transduction	3	*03P001, 05P001, 07A005*	Deletions	Mad^{10}	
kuzbanian	*kuz*	CG7147	*ADAM10*	Protease	Notch pathway	7	*02C041, 02P050, 04C518, 05C069, 05FB, 05C055, 05P027*	Deletions	$kuz^{e29\text{-}4}$	
neuralized	*neur*	CG11988	*NeurL1B*	Zn finger, RING-type	Notch pathway	1	*13P010*	Deletions	$neur^{1}$	
brain tumor	*brat*	CG10719	*TRIM3*	NHL, Zinc finger, B-box	asymmetric cell division, translation control	1	*05P009*	WGS	$brat^{1}$	
miranda	*mira*	CG12249	*SLMAP*		Myosin binding, asymmetric division	1	*11A017*	WGS	$mira^{L44}$	
dacapo	*dap*	CG1772	*Cdkn1a/1b/1c*	Cyclin inhibitor	Cell cycle	4	*02P040, 04P008, 05P025, 05P020*	Deletions	dap^{9454}	
Cyclin E	*CycE*	CG3928	*CCNE2*	Cyclin	Cell cycle	3	*02C043, 03F083, 05P024*	WGS	$CycE^{AR95}$	
Cyclin T	*CycT*	CG6292	*CCNT1*	Cyclin	Cell cycle	1	*11A005*	Deletions	$CycT^{5\text{-}HA\text{-}2393}$	
E2f transcription factor	*E2f*	CG6376	*E2F3*	Winged helix-turn-helix	Cell cycle	1	*09C008*	Deletions	$E2f^{87172}$	
CAP-D2 condensin subunit	*Cap-D2*	CG1911	*NCAPD2*	Armadillo-type fold	Mitotic chromosome condensation	1	*09C106*	WGS	$Dcap\text{-}D2^{f03381}$	59393
gluon	*glu*	CG11397	*SMC4*	SMC flexible hinge	Mitotic chromosome condensation	1	*04C205*	Deletions	glu^{k08819}	59394
sticky	*sti*	CG10522	*CIT*	S/T kinase domain	Cytokinesis	1	*12C001*	WGS	sti^{3}	59398
Regulator of chromosome condensation 1 ortholog	*Rcc1 (Bj1)*	CG10480	*RCC1*	RCC1 repeats	Chromatin binding	2	*08P004, 08P014*	Deletions	$RCC1^{FF32}$	
archipelago	*ago*	CG15010	*FBXW7*	F-box, WD40 repeat	Ubiquitin-protein ligase activity	1	*12A021*	WGS	ago^{1}	
peanuts	*pea*	CG8241	*DHX8*	Helicase, DEAH box	mRNA splicing	4	*01P030, 03F052, 05C120, 05P031*	WGS, Deletions	pea^{1}	59381
pre-mRNA processing factor 8	*Prp8*	CG8877	*PRPF8*	PROCT domain	mRNA splicing	1	*03F047*	WGS, Deletions	$Prp8^{2e1}$	59382
lethal(3)72Ab	*l(3)72Ab*	CG5931	*Brr2*	Helicase, DEAH box	mRNA splicing	3	*09C117, 13A036, 13C040*	Deletions	$l(3)72Ab^{e03171}$	59383, 59384
jhl-1	*jhl-1*	CG3298	*ELAC2*	tRNase Z endonuclease	RNA processing and transport	1	*03P028*	WGS	$jhl\text{-}1^{MI11532}$	59395
18 wheeler	*18w*	CG8896	*Slit homolog 1*	Toll-like receptor	Signaling	1	*03F247*	Deletions	$18w^{Delta7\text{-}35}$	59387
Notum	*Notum*	CG13076	*Notum*	PAE superfamily	Wnt pathway	1	*10A008*	WGS	$Notum^{72Da\text{-}1}$	
myopic	*mop*	CG9311	*PTPN23*	BRO-domain, phosphatase	tyrosine phosphatase	1	*13A023*	WGS	$mop^{EY06090}$	59392
muscle wasted	*mute*	CG34415	*GON-4-like*	Homeodomain-like	DNA-binding	2	*03P101, 05FH*	Deletions	$mute^{1281}$	59390, 59391
Nucleoporin 358kD	*Nup358*	CG11856	*RANBP2*	RAN binding domain	Nuclear import	2	*11P014, 12A002*	WGS	*Df(3R)FDD-0247627 Df(3R)FDD-0089346*	59396
cAMP-dependent protein kinase R1	*Pka-R1*	CG42341	*PRKAR1A*	Cyclic nucleotide-binding	cAMP-depdendent protein kinase regulator	1	*12C042*	WGS	$Pka\text{-}R1^{MB04145}$	59397
Surfeit 6	*Surf6*	CG4510	*SURF6*	ApoLp-III	Heme transporter	1	*12C004*	WGS	$Surf6^{C329}$	59399
Total # genes:	***43***				***Total # alleles:***	**79**				

A total of 79 mutants were mapped down to 43 genes. A number of alleles were identified in genes for which no apparent null alleles existed, and these were deposited at the Bloomington Drosophila Stock Center. For a number of genes, we have found no previous reports regarding their role in CNS development (red text). $18w^{037247}$ was lethal over deficiencies for the region, but not lethal over $18w^{Delta7\text{-}35}$. However, the $18w^{037247}/18w^{Delta7\text{-}35}$ allelic combination did show the expected phenotype. For *Nup358* and *lbe* no alleles were available. However, $Nup358^{12A002}$ and lbe^{12C005} were mapped to 20- and 50-kb regions, respectively, and in these intervals we did not identify any heterozygous SNPs, other than the ones in *Nup358* or *lbe* (data not shown). For *CG2469* (*Ctr9*), no alleles were available, but ongoing work verified that the $CG2469^{12P023}$ allele could be rescued by a *UAS-CG2469* transgene (S. Bahrampour and S. Thor, unpublished observation).

chromatin-remodeling complex and has been implicated in a wide range of processes, including control of proliferation (Wilson and Roberts 2011; Romero and Sanchez-Cespedes 2014). Intriguingly, recent studies demonstrated that the *Drosophila* SWI/SNF complex is involved in development of larval NBs (Eroglu *et al.* 2014). Our marker analysis showed a rather subtle defect in differentiation, with a normal number of Ap cluster neurons, albeit a strong loss of FMRFa (Table 1).

CG2469 is the *Drosophila* ortholog of mammalian Ctr9, a key component of the Paf1 complex (Paf1C), which interacts with RNA Polymerase II and is involved in a number of gene expression events, including Histone H3 trimethylation (Jaehning 2010). Our isolated *CG2469* allele displayed a complex effect on Ap clusters, with loss of FMRFa but extra numbers of Eya-expressing neurons (Table 1).

Ap4/FMRFa cell fate

Previous studies have identified a number of cell fate determinants acting to specify Ap4/FMRFa cell fate (Benveniste *et al.* 1998; van Meyel *et al.* 2000; Allan *et al.* 2003, 2005; Hewes *et al.* 2003; Marques *et al.* 2003; Miguel-Aliaga *et al.* 2004; Baumgardt *et al.* 2007, 2009). Of these genes, we isolated new alleles for *collier* (*col*) (FlyBase *knot*) (Figure 4, I, L, and O) and *eyes absent* (*eya*), encoding a COE HLH transcription factor and a transcription cofactor and nuclear phosphatase, respectively (Table 2). As anticipated from previous studies, these alleles displayed a loss of Ap4 cell markers (Table 1).

Axonal retrograde transport/BMP signaling

The fact that the Ap4 neuron is critically dependent upon the retrograde BMP signal from the axonal target for FMRFa expression, together with its unique axonal trajectory to the DNH (Figure 1C), raised the possibility that this screen would reveal a multitude of novel genes affecting axon pathfinding, axon transport, and TGFβ/BMP signaling. Defects in these processes would be readily visible by loss of pMad, since access to the TGFβ/BMP ligands—present in the periphery—and transport of pMad to the nucleus requires proper pathfinding, transport, and signal transduction (Allan *et al.* 2003; Marques *et al.* 2003). On this note, we isolated mutants with global pMad staining reduction, all of which mapped to previously known genes: the BMP ligand-encoding gene *gbb* and the downstream effector *Mad* (Figure 4, J, M, and P; Table 2). However, we did not identify any other obvious components of TGFβ/BMP signaling.

Notch signaling

Among the mutants that displayed additional Ap neurons, a number were mapped to two genes in the Notch pathway: *neuralized* (*neur*) and *kuzbanian* (*kuz*) (Table 2; Figure 5, A–C) (Bray 2006). The Notch pathway is known for acting early during NB delamination, as well as for separating sibling cell fates in the developing *Drosophila* VNC (Hartenstein and Wodarz 2013). The identification in the EMS screen of the Notch pathway as affecting Ap cell numbers previously prompted us to address in more detail the role of Notch. This revealed that Notch signaling acts specifically to trigger the type I > 0 switch in daughter cell proliferation mode (Ulvklo *et al.* 2012).

Cell cycle genes

Recent studies of NB lineage progression in the VNC involved screening specifically for proliferation phenotypes of 21 of the most prominent cell cycle genes. This revealed striking proliferation defects in only a small subset of genes, which we presume is due to the maternal loading of many cell cycle genes. Hence many cell cycle genes are neither critically transcriptionally regulated in the embryo nor zygotically essential (Baumgardt *et al.* 2014). Our unbiased EMS screen herein revealed the same genes as critical players in embryonic VNC development: *dacapo* (*dap*), *Cyclin E* (*CycE*), and *E2f* (Table 2). However, our unbiased screen also identified mutations in the *Cyclin T* (*CycT*), which was not tested in the previous study (Baumgardt *et al.* 2014) (Table 2). These mutants generated predictable phenotypes, with an increase of Ap cluster cells in *dap* (the *Drosophila* ortholog of the mammalian $p21^{CIP1}/p27^{KIP1}/p57^{Kip2}$ CycE/Cdk1 inhibitors, encoded by the *Cdkn1a/b/c* genes, respectively), and a loss of Eya cells in *CycE*, *CycT*, and *E2f* (Table 1). We identified a mutation for *CycE* in two alleles and found nonsense mutations in both (Table S1).

Asymmetric division

Proper lineage progression in NBs is critically dependent upon asymmetric cell division, wherein a number of proteins are selectively distributed either to the NB or to the daughter cell (Sousa-Nunes and Somers 2013). NB components repress differentiation and promote proliferation, while, conversely, daughter components promote differentiation and repress proliferation. In line with this, novel alleles of *miranda* (*mira*) (Figure 5D) displayed loss of Ap cluster markers, and novel alleles of *brain tumor* (*brat*) displayed extra Ap cluster markers, as would be expected from their roles in asymmetric cell division (Table 1 and Table 2) (Knoblich 2008). We identified the mutations for *mira* and *brat* as nonsense mutations (Table S1).

Chromosome condensation and cytokinesis

Proper chromosome condensation during cytokinesis requires the packaging activity of two well-conserved condensin multiprotein complexes, I and II (Hirano 2012). The condensin I complex contains several well-conserved proteins, two of which were isolated in the screen: *Cap-D2 condensin subunit* (*Cap-D2*; Table 2) and *gluon* (*glu*; also known as *SMC4*) . We identified the mutation for *Cap-D2* and found a nonsense mutation (Table S1). Previous studies have revealed that both *glu* and *Cap-D2* are important for sister-chromatid resolution during mitosis (Steffensen *et al.* 2001; Savvidou *et al.* 2005). In line with a role for these genes in proper mitosis, we find that both genes display a loss of Ap4 and Ap cluster neurons (Table 1). We also isolated one allele for the *sticky* (*sti*) kinase, the fly ortholog of the mammalian Citron kinase, which has been shown to play key roles during cytokinesis (Table 2) (D'Avino *et al.* 2004; Shandala *et al.* 2004). We identified the mutation for *sti* and found a nonsense mutation (Table S1).

Proteolysis

Most, if not all, of the cell cycle proteins identified as being important for proper cell cycle control during *Drosophila* embryonic CNS development are extensively controlled at the level of proteolysis (Clarke 2002; Yamasaki and Pagano 2004). In line with this, we isolated a new allele in the *archipelago* (*ago*) gene (Table 2), the fly ortholog of mammalian Fbxw7 (Moberg *et al.* 2004). We identified the mutation for *ago* and found a G1091D substitution, which affects a residue in the WD40 domain, conserved in the human Fbxw7 protein (Table S1; not shown). Ago/Fbxw7 is known to be critical for degradation of several proteins, including CycE (Nicholson *et al.* 2011; Davis *et al.* 2014), likely explaining the observed phenotype of additional Ap cells in this mutant (Table 1).

RNA processing

Transcriptome analysis points to a greater extent of tissue- and cell-specific RNA splicing than was previously appreciated, and in the fly genome the majority of genes have now been found to generate alternate transcripts (Brown *et al.* 2014). However, the mechanisms underlying alternate splicing are still not well understood (Fu and Ares 2014). We isolated four genes involved in mRNA splicing and one involved in RNA processing and transport. *peanuts* (*pea*) and *lethal(3)72Ab* (*l(3)72Ab*) encode RNA helicases. *pea* is the fly ortholog of mammalian *DHX8* and yeast *prp22*, while *l(3)72Ab* encodes the ortholog of mammalian *Brr2*. *pre-mRNA processing factor 8* (*Prp8*) encodes a PROCT domain protein and is the ortholog of mammalian *PRPF8*. *jhI-1* encodes a tRNase Z endonuclease and is the ortholog of mammalian *ELAC2* (Table 2). The role of these genes during embryonic development is not well understood. We identified the mutation for *pea*, *Prp8*, and *jhI-1* and found a S747L substation in Pea and nonsense mutations in *Prp8* and *jhI-1* (Table S1). The S747L mutation in Pea affects a residue in the DEAD-like domain and is conserved in the human DHX8 protein (not shown). *pea* and *l(3)72Ab* display loss of FMRFa and pMad, but normal Eya, while *Prp8* shows loss of FMRFa with extra Eya, and *jhI-1* shows extra FMRFa and Eya (Table 1).

Toll, Wnt, and EGFR signaling

In addition to the TGFβ/BMP-signaling pathway, we identified three genes involved in other signaling pathways: *Notum*, *myopic* (*mop*), and *18 wheeler* (*18w*) (Table 2). The *Notum* and *mop* alleles were sequenced and found to contain nonsense mutations (Table S1). *18w* encodes a Toll-like receptor and has been found to be important for imaginal disc developmental and antibacterial defense (Eldon *et al.* 1994; Williams *et al.* 1997). The *18w* allele that we isolated displayed loss of Ap cell markers (Table 1). *Notum* encodes an α/β-hydrolase with similarity to pectin acetylesterases from plants and has been demonstrated to affect the gradient of the Wingless (Wg) ligand in the developing wing by modifying cell-surface proteoglycans (Giraldez *et al.* 2002). We found a loss of Ap markers in *Notum* (Table 1). *mop* encodes a tyrosine phosphatase, found to promote EGFR signaling in imaginal discs (Miura *et al.* 2008), and we observed loss of Ap markers in *mop* (Table 1).

Uncategorized genes identified

muscle wasted (*mute*) encodes a divergent putative transcription protein, part of the histone locus body complex, and has been shown to be important for embryonic muscle development (Bulchand *et al.* 2010) (Table 2). We observed loss of Ap markers in *mute* (Table 1). *cAMP-dependent protein kinase R1* (*PKA-R1*) (Figure 5D) encodes a regulatory subunit of the PKA complex (Kalderon and Rubin 1988; Park *et al.* 2000). *PKA-R1* plays diverse roles in *Drosophila*, ranging from oocyte patterning to learning and memory (Goodwin *et al.* 1997; Yoshida *et al.* 2004). We observed a complex marker profile in PKA-R1 with variable loss or gain of FMRFa, gain of Dimm, and occasional extra pMad (Figure 5D; Table 1). *Surfeit 6* (*Surf6*) encodes a putative nucleic-acid-binding protein, with no known loss-of-function role in *Drosophila* (Table 2). The mammalian ortholog Surf6 was found to be part of the nucleolar matrix and may bind both RNA and DNA (Magoulas *et al.* 1998). We observed extra FMRFa, Eya, and pMad expression in *Surf6* (Table 1).

Finally, we isolated the Ran GTPase guanine-nucleotide exchange factor *Regulator of chromosome condensation 1 ortholog* (*RCC1*; also known as *Bj1*) (Table 2). The translocation of RNA and proteins through the nuclear pore complex critically depends upon Ran GTPase (Guttler and Gorlich 2011). *Bj1* was previously found to be important for embryonic CNS development and for nuclear protein import (Shi and Skeath 2004). More recently, *Bj1* was found to act in larval NBs, controlling NB numbers and preventing differentiation, likely by controlling nuclear export of the Prospero transcription factor (Joy *et al.* 2014). In line with these findings, our *Bj1* allele displayed loss of Ap cluster markers analyzed (Table 1). We also isolated another gene involved in Ran biology: *Nucleoporin 358kD* (*Nup358*), which encodes a complex multi-domain protein and is the fly ortholog of Ran Binding Protein 2, found to control nuclear mRNA export (Table 2) (Forler *et al.* 2004). No loss-of-function analysis has been published on this gene before. We observed loss of Ap markers in *Nup358* (Table 1). We identified the mutation for *Nup358*, *PKA-R1*, and *Surf6* and found nonsense mutations in *Nup358* and *Surf6* (Table S1). Surprisingly, *PKA-R1* had two missense mutations in the ORF (Table S1).

Discussion

Forward genetics is a powerful method to identify novel genes and, by extension, biological processes that have an impact on a phenotype of interest. By the use of an *FMRFa-eGFP* reporter transgene we could extensively screen the genome for perturbations of FMRFa expression and Ap4 specification and thereby identify genes acting at many levels of NB5-6T development (Figure 6). Because of the powerful genetic tools available, *i.e.*, the *FMRFa-eGFP* transgene and the *hs-hid* balancer chromosomes, the mutagenesis and screening was relatively straightforward. In contrast, the mapping of the identified mutants was a labor-intensive task. During the initial phases of this screen, a novel approach of transposon mapping was tested, but was nonconclusive. In addition, SNP mapping was considered, but given the amount of work involved in generating a large battery of recombinant substocks, this approach was not employed. Instead, deficiency mapping against the Bloomington Deficiency Kit proved to be a straightforward and reliable approach for identifying the genomic region affected in many mutants. Initially, we mapped mutants based upon the assumption that the gene affecting *FMRFa-eGFP* would cause lethality, which is comparatively straightforward, since only the adult balancer markers are scored. However, in a number of cases, the mutation affecting the *FMRFa-eGFP* expression was not lethal, and in some of these cases we chose to conduct embryonic phenotypic mapping against the deficiency kit. This is more labor intensive, since it involves crossing the mutant to all deficiencies for that chromosome and analyzing eGFP expression in embryo collections. Hence, a number of nonlethal mutants were not pursued, and this may have skewed the type of genes that were identified.

The use of next-generation sequencing for identifying EMS-induced mutations has been previously used in both *Drosophila* and *Caenorhabditis elegans* (Smith *et al.* 2008; Blumenstiel *et al.* 2009; Haelterman *et al.* 2014) and is coming to the forefront as the method of choice for mapping of mutations in genetic screens (Schneeberger 2014). Blumenstiel and colleagues show that a 45-mM dose of EMS causes an average of 11 mutations affecting coding sequences per chromosome (Blumenstiel *et al.* 2009). We did not quantify the average number of EMS-induced changes per chromosome in our screen, but we identified several missense and nonsense mutations in each mutant and did indeed have to test an average of seven candidate genes per mutant pair to identify the gene affected. Because missense and nonsense mutations account for only a small fraction of actual

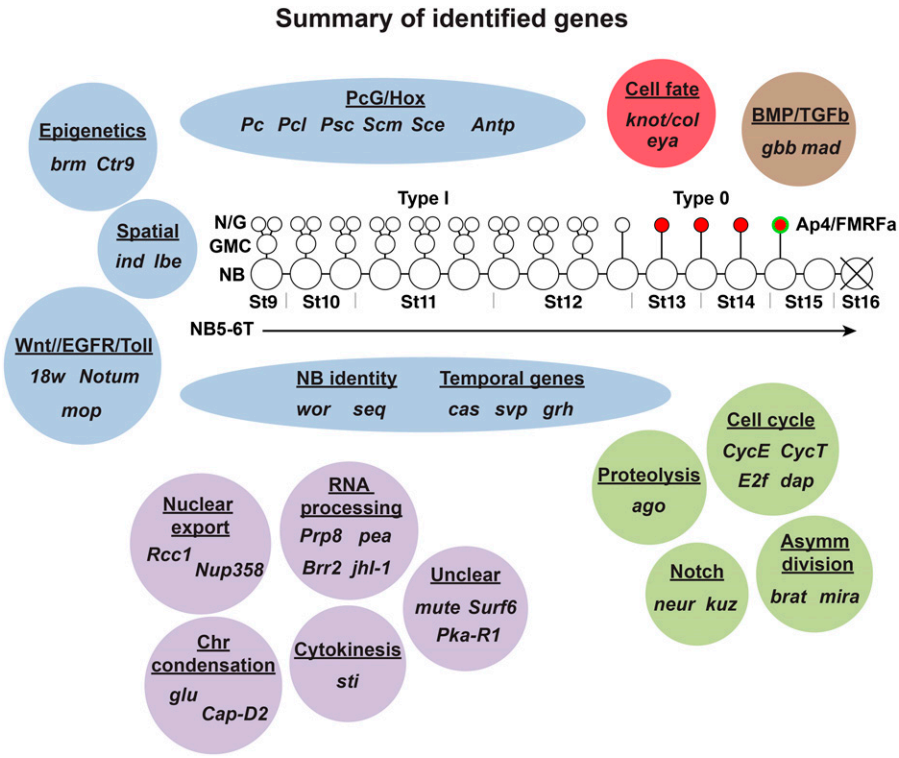

Figure 6 Summary of genes identified in the screen affecting the NB5-6T lineage. The NB5-6T lineage and the four Ap neurons (red) are depicted at the center with the Ap4/FMRFa cell (green). Based upon previous studies and gene category, we grouped most of the genes identified in the screen in broadly defined categories (blue): these include epigenetic factors, spatial cues, signaling cues, NB identity, and temporal cues, as well as PcG/Hox cues. Two genes are known to specify Ap4 cell fate (red), and two genes control TGFβ/BMP retrograde signaling (brown). Genes involved in cell cycle genes, proteolysis, asymmetric cell division, and Notch signaling (green) all play roles in controlling precise proliferation of NBs and daughters. The categorization of some genes identified requires further study (purple). These are genes involved in nuclear export, RNA processing, chromosome condensation, cytokinesis, and three genes (*mute*, *Surf6*, and *Pka-R1*) that are not readily categorized.

mutations, our EMS mutagenesis appears to have been quite robust. Nevertheless, the combination of a restricted phenotypic marker, high-throughput screening, and a straightforward WGS approach would be a promising way to cover the genome and reach close to 100% saturation.

Given the requirement of the retrograde TGFβ/BMP signal for FMRFa expression, we anticipated finding many genes involved in axon pathfinding, axon transport, and TGFβ/BMP signaling. However, to our surprise we re-identified only two TGFβ/BMP components, *gbb* and *mad*, and no obvious axon pathfinding or axon transport genes. We also anticipated identifying novel temporal transcription factors. This notion was based upon the facts that this type of gene function has not been systematically screened for previously and that there are many transcription factors encoded by the fly genome, the majority of which have unknown roles during development. Indeed, we re-identified the temporal genes *cas* and *grh*. In addition, we identified *svp*, and detailed studies revealed that it plays a second, late role in the NB5-6T lineage (Benito-Sipos *et al.* 2011). However, no other obvious temporal genes were identified, although a more detailed analysis may of course reveal genes playing such roles among the unmapped mutants that we isolated. Similarly, we anticipated identifying proteolysis genes, since genes encoding these types of proteins (*e.g.*, E3/E2-ligases and F-box proteins) are plentiful in the genome, the vast majority of which have unknown roles during development. However, our screen re-identified only the proteolysis gene *ago*. There may be several reasons why we failed to identify novel genes in these categories. First, many nonlethal alleles were not pursued, and such genes may be present among unmapped genes. Second, many genes in the fly genome are maternally loaded into the embryo, which often precludes them from being isolated in a classic F_1 embryonic screen. Third, the screen was conducted for only the second and third chromosomes, and, judging from the number of alleles isolated for each identified gene (Table 2), was far from saturated for these chromosomes. Hence, a more extensive screen may have identified novel components in the abovementioned pathways.

Our screen resulted in the identification of 43 genes necessary for Ap4/FMRFa cell specification. Strikingly, all genes identified have clear predicted human orthologs (Table 2), and this may well be due to that our mapping efforts were primarily aimed toward identifying the lethal genes in the collection, since conserved genes are more frequently essential than nonconserved genes (Yamamoto *et al.* 2014). While many genes were previously known to play roles during CNS development, 16 genes were not: *e.g.*, *pea*, *Prp8*, *Brr2*, *jhI-1*, *18w*, *Notum*, *mop*, *mute*, *Nup358*, *Pka-R1* and *Surf6* (Table 2, red). For several of these genes, strong or null alleles were not previously identified, and therefore a number of stocks have been deposited at the Bloomington Drosophila Stock Center (Table 2). It is possible that the high resolution of the reporter and the detailed knowledge of its context provided us with the opportunity to discover new actions of these genes in the CNS. Further characterization of the genes identified in the screen will hopefully give new insights into stem cell competence, cell fate specification, and other aspects of neural development.

Acknowledgments

We thank the Developmental Studies Hybridoma bank at the University of Iowa; the Bloomington and Kyoto Drosophila Stock Centers; Kevin Cook, Ed Laufer, Rob White, K. Wharton, P. H. Taghert, A. Vincent, F. Diaz-Benjumea, W. Odenwald, I. Miguel-Aliaga, G. Technau, K. Moberg, R. Urbach, and K. Jagla; Douglas Allan and Bassem Hassan for thoughtful comments on the manuscript; Malin Barvén Trollvik, Sabina Lundblad, Maria Baytar, Shoko Kasuya, Johan Larsen, and Annika Starkenberg for their aid in the mapping of mutants; and Helen Ekman, Carolin Jonsson, and Olivia Forsberg for excellent technical assistance.

Literature Cited

Allan, D. W., and S. Thor, 2015 Transcriptional selectors, masters, and combinatorial codes: regulatory principles of neural subtype specification. Wiley Interdiscip. Rev. Dev. Biol. DOI: 10.1002/wdev.191.

Allan, D. W., S. E. Pierre, I. Miguel-Aliaga, and S. Thor, 2003 Specification of neuropeptide cell identity by the integration of retrograde BMP signaling and a combinatorial transcription factor code. Cell 113: 73–86.

Allan, D. W., D. Park, S. E. St Pierre, P. H. Taghert, and S. Thor, 2005 Regulators acting in combinatorial codes also act independently in single differentiating neurons. Neuron 45: 689–700.

Andrews, H. K., N. Giagtzoglou, S. Yamamoto, K. L. Schulze, and H. J. Bellen, 2009 Sequoia regulates cell fate decisions in the external sensory organs of adult Drosophila. EMBO Rep. 10: 636–641.

Ashraf, S. I., and Y. T. Ip, 2001 The Snail protein family regulates neuroblast expression of inscuteable and string, genes involved in asymmetry and cell division in Drosophila. Development 128: 4757–4767.

Ashraf, S. I., X. Hu, J. Roote, and Y. T. Ip, 1999 The mesoderm determinant snail collaborates with related zinc-finger proteins to control Drosophila neurogenesis. EMBO J. 18: 6426–6438.

Barolo, S., L. A. Carver, and J. W. Posakony, 2000 GFP and beta-galactosidase transformation vectors for promoter/enhancer analysis in Drosophila. Biotechniques 29: 726, 728, 730, 732.

Baumgardt, M., I. Miguel-Aliaga, D. Karlsson, H. Ekman, and S. Thor, 2007 Specification of neuronal identities by feedforward combinatorial coding. PLoS Biol. 5: 295–308.

Baumgardt, M., D. Karlsson, J. Terriente, F. J. Diaz-Benjumea, and S. Thor, 2009 Neuronal subtype specification within a lineage by opposing temporal feed-forward loops. Cell 139: 969–982.

Baumgardt, M., D. Karlsson, B. Y. Salmani, C. Bivik, R. B. MacDonald *et al.*, 2014 Global programmed switch in neural daughter cell proliferation mode triggered by a temporal gene cascade. Dev. Cell 30: 192–208.

Benito-Sipos, J., C. Ulvklo, H. Gabilondo, M. Baumgardt, A. Angel *et al.*, 2011 Seven up acts as a temporal factor during two different stages of neuroblast 5–6 development. Development 138: 5311–5320.

Benveniste, R. J., S. Thor, J. B. Thomas, and P. H. Taghert, 1998 Cell type-specific regulation of the Drosophila FMRF-NH2 neuropeptide gene by Apterous, a LIM homeodomain transcription factor. Development 125: 4757–4765.

Birkholz, O., O. Vef, A. Rogulja-Ortmann, C. Berger, and G. M. Technau, 2013 Abdominal-B and caudal inhibit the formation of specific neuroblasts in the Drosophila tail region. Development 140: 3552–3564.

Blumenstiel, J. P., A. C. Noll, J. A. Griffiths, A. G. Perera, K. N. Walton *et al.*, 2009 Identification of EMS-induced mutations in *Drosophila melanogaster* by whole-genome sequencing. Genetics 182: 25–32.

Bossing, T., G. Udolph, C. Q. Doe, and G. M. Technau, 1996 The embryonic central nervous system lineages of Drosophila melanogaster. I. Neuroblast lineages derived from the ventral half of the neuroectoderm. Dev. Biol. 179: 41–64.

Bray, S. J., 2006 Notch signalling: a simple pathway becomes complex. Nat. Rev. Mol. Cell Biol. 7: 678–689.

Brenman, J. E., F. B. Gao, L. Y. Jan, and Y. N. Jan, 2001 Sequoia, a tramtrack-related zinc finger protein, functions as a pan-neural regulator for dendrite and axon morphogenesis in Drosophila. Dev. Cell 1: 667–677.

Broadus, J., J. B. Skeath, E. P. Spana, T. Bossing, G. Technau *et al.*, 1995 New neuroblast markers and the origin of the aCC/pCC neurons in the Drosophila central nervous system. Mech. Dev. 53: 393–402.

Brody, T., and W. F. Odenwald, 2000 Programmed transformations in neuroblast gene expression during Drosophila CNS lineage development. Dev. Biol. 226: 34–44.

Brown, J. B., N. Boley, R. Eisman, G. E. May, M. H. Stoiber *et al.*, 2014 Diversity and dynamics of the Drosophila transcriptome. Nature 512: 393–399.

Bulchand, S., S. D. Menon, S. E. George, and W. Chia, 2010 Muscle wasted: a novel component of the Drosophila histone locus body required for muscle integrity. J. Cell Sci. 123: 2697–2707.

Cai, Y., W. Chia, and X. Yang, 2001 A family of snail-related zinc finger proteins regulates two distinct and parallel mechanisms that mediate Drosophila neuroblast asymmetric divisions. EMBO J. 20: 1704–1714.

Clarke, D. J., 2002 Proteolysis and the cell cycle. Cell Cycle 1: 233–234.

D'Avino, P. P., M. S. Savoian, and D. M. Glover, 2004 Mutations in sticky lead to defective organization of the contractile ring during cytokinesis and are enhanced by Rho and suppressed by Rac. J. Cell Biol. 166: 61–71.

Davis, R. J., M. Welcker, and B. E. Clurman, 2014 Tumor suppression by the Fbw7 ubiquitin ligase: mechanisms and opportunities. Cancer Cell 26: 455–464.

De Graeve, F., T. Jagla, J. P. Daponte, C. Rickert, B. Dastugue *et al.*, 2004 The ladybird homeobox genes are essential for the specification of a subpopulation of neural cells. Dev. Biol. 270: 122–134.

Doe, C. Q., 1992 Molecular markers for identified neuroblasts and ganglion mother cells in the Drosophila central nervous system. Development 116: 855–863.

Eldon, E., S. Kooyer, D. D'Evelyn, M. Duman, P. Lawinger *et al.*, 1994 The Drosophila 18 wheeler is required for morphogenesis and has striking similarities to Toll. Development 120: 885–899.

Eroglu, E., T. R. Burkard, Y. Jiang, N. Saini, C. C. Homem *et al.*, 2014 SWI/SNF complex prevents lineage reversion and induces temporal patterning in neural stem cells. Cell 156: 1259–1273.

Forler, D., G. Rabut, F. D. Ciccarelli, A. Herold, T. Kocher *et al.*, 2004 RanBP2/Nup358 provides a major binding site for NXF1-p15 dimers at the nuclear pore complex and functions in nuclear mRNA export. Mol. Cell. Biol. 24: 1155–1167.

Francis, N. J., A. J. Saurin, Z. Shao, and R. E. Kingston, 2001 Reconstitution of a functional core polycomb repressive complex. Mol. Cell 8: 545–556.

Fu, X. D., and M. Ares, Jr.., 2014 Context-dependent control of alternative splicing by RNA-binding proteins. Nat. Rev. Genet. 15: 689–701.

Gerhold, A. R., D. J. Richter, A. S. Yu, and I. K. Hariharan, 2011 Identification and characterization of genes required for compensatory growth in *Drosophila*. Genetics 189: 1309–1326.

Giraldez, A. J., R. R. Copley, and S. M. Cohen, 2002 HSPG modification by the secreted enzyme Notum shapes the Wingless morphogen gradient. Dev. Cell 2: 667–676.
Goodwin, S. F., M. Del Vecchio, K. Velinzon, C. Hogel, S. R. Russell *et al.*, 1997 Defective learning in mutants of the Drosophila gene for a regulatory subunit of cAMP-dependent protein kinase. J. Neurosci. 17: 8817–8827.
Grosskortenhaus, R., B. J. Pearson, A. Marusich, and C. Q. Doe, 2005 Regulation of temporal identity transitions in Drosophila neuroblasts. Dev. Cell 8: 193–202.
Guttler, T., and D. Gorlich, 2011 Ran-dependent nuclear export mediators: a structural perspective. EMBO J. 30: 3457–3474.
Haelterman, N. A., L. Jiang, Y. Li, V. Bayat, H. Sandoval *et al.*, 2014 Large-scale identification of chemically induced mutations in Drosophila melanogaster. Genome Res. 24: 1707–1718.
Hartenstein, V., and A. Wodarz, 2013 Initial neurogenesis in Drosophila. Wiley Interdiscip. Rev. Dev. Biol. 2: 701–721.
Hewes, R. S., D. Park, S. A. Gauthier, A. M. Schaefer, and P. H. Taghert, 2003 The bHLH protein Dimmed controls neuroendocrine cell differentiation in Drosophila. Development 130: 1771–1781.
Hirano, T., 2012 Condensins: universal organizers of chromosomes with diverse functions. Genes Dev. 26: 1659–1678.
Isshiki, T., B. Pearson, S. Holbrook, and C. Q. Doe, 2001 Drosophila neuroblasts sequentially express transcription factors which specify the temporal identity of their neuronal progeny. Cell 106: 511–521.
Jaehning, J. A., 2010 The Paf1 complex: Platform or player in RNA polymerase II transcription? Biochim. Biophys. Acta 1799: 379–388.
Jiang, C., E. H. Baehrecke, and C. S. Thummel, 1997 Steroid regulated programmed cell death during Drosophila metamorphosis. Development 124: 4673–4683.
Joy, T., K. Hirono, and C. Q. Doe, 2014 The RanGEF Bj1 promotes prospero nuclear export and neuroblast self-renewal. Dev. Neurobiol. 75: 485–493.
Kalderon, D., and G. M. Rubin, 1988 Isolation and characterization of Drosophila cAMP-dependent protein kinase genes. Genes Dev. 2: 1539–1556.
Karlsson, D., M. Baumgardt, and S. Thor, 2010 Segment-specific neuronal subtype specification by the integration of anteroposterior and temporal cues. PLoS Biol. 8: e1000368.
Knoblich, J. A., 2008 Mechanisms of asymmetric stem cell division. Cell 132: 583–597.
Koundakjian, E. J., D. M. Cowan, R. W. Hardy, and A. H. Becker, 2004 The Zuker collection: a resource for the analysis of autosomal gene function in *Drosophila melanogaster*. Genetics 167: 203–206.
Magoulas, C., O. V. Zatsepina, P. W. Jordan, E. G. Jordan, and M. Fried, 1998 The SURF-6 protein is a component of the nucleolar matrix and has a high binding capacity for nucleic acids in vitro. Eur. J. Cell Biol. 75: 174–183.
Marques, G., T. E. Haerry, M. L. Crotty, M. Xue, B. Zhang *et al.*, 2003 Retrograde Gbb signaling through the Bmp type 2 receptor wishful thinking regulates systemic FMRFa expression in Drosophila. Development 130: 5457–5470.
McDonald, J. A., S. Holbrook, T. Isshiki, J. Weiss, C. Q. Doe *et al.*, 1998 Dorsoventral patterning in the Drosophila central nervous system: the vnd homeobox gene specifies ventral column identity. Genes Dev. 12: 3603–3612.
Miguel-Aliaga, I., D. W. Allan, and S. Thor, 2004 Independent roles of the dachshund and eyes absent genes in BMP signaling, axon pathfinding and neuronal specification. Development 131: 5837–5848.
Miura, G. I., J. Y. Roignant, M. Wassef, and J. E. Treisman, 2008 Myopic acts in the endocytic pathway to enhance signaling by the Drosophila EGF receptor. Development 135: 1913–1922.
Moberg, K. H., A. Mukherjee, A. Veraksa, S. Artavanis-Tsakonas, and I. K. Hariharan, 2004 The Drosophila F box protein archipelago regulates dMyc protein levels in vivo. Curr. Biol. 14: 965–974.
Nicholson, S. C., B. N. Nicolay, M. V. Frolov, and K. H. Moberg, 2011 Notch-dependent expression of the archipelago ubiquitin ligase subunit in the Drosophila eye. Development 138: 251–260.
Park, S. K., S. A. Sedore, C. Cronmiller, and J. Hirsh, 2000 Type II cAMP-dependent protein kinase-deficient Drosophila are viable but show developmental, circadian, and drug response phenotypes. J. Biol. Chem. 275: 20588–20596.
Pearson, B. J., and C. Q. Doe, 2004 Specification of temporal identity in the developing nervous system. Annu. Rev. Cell Dev. Biol. 20: 619–647.
Pereira, F. A., M. J. Tsai, and S. Y. Tsai, 2000 COUP-TF orphan nuclear receptors in development and differentiation. Cell. Mol. Life Sci. 57: 1388–1398.
Romero, O. A., and M. Sanchez-Cespedes, 2014 The SWI/SNF genetic blockade: effects in cell differentiation, cancer and developmental diseases. Oncogene 33: 2681–2689.
Savvidou, E., N. Cobbe, S. Steffensen, S. Cotterill, and M. M. Heck, 2005 Drosophila CAP-D2 is required for condensin complex stability and resolution of sister chromatids. J. Cell Sci. 118: 2529–2543.
Schmid, A., A. Chiba, and C. Q. Doe, 1999 Clonal analysis of Drosophila embryonic neuroblasts: neural cell types, axon projections and muscle targets. Development 126: 4653–4689.
Schmidt, H., C. Rickert, T. Bossing, O. Vef, J. Urban *et al.*, 1997 The embryonic central nervous system lineages of Drosophila melanogaster. II. Neuroblast lineages derived from the dorsal part of the neuroectoderm. Dev. Biol. 189: 186–204.
Schneeberger, K., 2014 Using next-generation sequencing to isolate mutant genes from forward genetic screens. Nat. Rev. Genet. 15: 662–676.
Schneider, L. E., M. S. Roberts, and P. H. Taghert, 1993 Cell type-specific transcriptional regulation of the Drosophila FMRFamide neuropeptide gene. Neuron 10: 279–291.
Shandala, T., S. L. Gregory, H. E. Dalton, M. Smallhorn, and R. Saint, 2004 Citron kinase is an essential effector of the Pbl-activated Rho signalling pathway in Drosophila melanogaster. Development 131: 5053–5063.
Shi, W. Y., and J. B. Skeath, 2004 The Drosophila RCC1 homolog, Bj1, regulates nucleocytoplasmic transport and neural differentiation during Drosophila development. Dev. Biol. 270: 106–121.
Skeath, J. B., 1999 At the nexus between pattern formation and cell-type specification: the generation of individual neuroblast fates in the Drosophila embryonic central nervous system. BioEssays 21: 922–931.
Skeath, J. B., and S. Thor, 2003 Genetic control of Drosophila nerve cord development. Curr. Opin. Neurobiol. 13: 8–15.
Smith, D. R., A. R. Quinlan, H. E. Peckham, K. Makowsky, W. Tao *et al.*, 2008 Rapid whole-genome mutational profiling using next-generation sequencing technologies. Genome Res. 18: 1638–1642.
Sousa-Nunes, R., and W. G. Somers, 2013 Mechanisms of asymmetric progenitor divisions in the Drosophila central nervous system. Adv. Exp. Med. Biol. 786: 79–102.
Steffensen, S., P. A. Coelho, N. Cobbe, S. Vass, M. Costa *et al.*, 2001 A role for Drosophila SMC4 in the resolution of sister chromatids in mitosis. Curr. Biol. 11: 295–307.
Ulvklo, C., R. Macdonald, C. Bivik, M. Baumgardt, D. Karlsson *et al.*, 2012 Control of neuronal cell fate and number by integration of distinct daughter cell proliferation modes with temporal progression. Development 139: 678–689.
van Meyel, D. J., D. D. O'Keefe, S. Thor, L. W. Jurata, G. N. Gill *et al.*, 2000 Chip is an essential cofactor for apterous in the regulation of axon guidance in Drosophila. Development 127: 1823–1831.

Williams, M. J., A. Rodriguez, D. A. Kimbrell, and E. D. Eldon, 1997 The 18-wheeler mutation reveals complex antibacterial gene regulation in Drosophila host defense. EMBO J. 16: 6120–6130.

Wilson, B. G., and C. W. Roberts, 2011 SWI/SNF nucleosome remodellers and cancer. Nat. Rev. Cancer 11: 481–492.

von Ohlen, T., and C. Q. Doe, 2000 Convergence of dorsal, dpp, and egfr signaling pathways subdivides the Drosophila neuroectoderm into three dorsal-ventral columns. Dev. Biol. 224: 362–372.

Yamamoto, S., M. Jaiswal, W. L. Charng, T. Gambin, E. Karaca *et al.*, 2014 A Drosophila genetic resource of mutants to study mechanisms underlying human genetic diseases. Cell 159: 200–214.

Yamasaki, L., and M. Pagano, 2004 Cell cycle, proteolysis and cancer. Curr. Opin. Cell Biol. 16: 623–628.

Yoshida, S., H. A. Muller, A. Wodarz, and A. Ephrussi, 2004 PKA-R1 spatially restricts Oskar expression for Drosophila embryonic patterning. Development 131: 1401–1410.

Communicating editor: H. J. Bellen

GENETICS

Supporting Information
www.genetics.org/lookup/suppl/doi:10.1534/genetics.115.178483/-/DC1

Novel Genes Involved in Controlling Specification of *Drosophila* FMRFamide Neuropeptide Cells

Caroline Bivik, Shahrzad Bahrampour, Carina Ulvklo, Patrik Nilsson, Anna Angel, Fredrik Fransson, Erika Lundin, Jakob Renhorn, and Stefan Thor

DOI: 10.1534/genetics.115.178483

Table S1. DNA sequence analysis of 24 mutants

DNA prepp	WGS company	WGS	Line	Chr	Gene	CG	Mutant DNA	# of reads	SNP %	DNA seq	Mutant aa
1	GATC Biotech	Illumina HiSeq 2000, Unpaired 100 bp, 30-50 M reads	*08A006*	3L							
1	GATC Biotech	Illumina HiSeq 2000, Unpaired 100 bp, 30-50 M reads	*09C106*	3R	*Cap-D2*	*CG1911*	544C>T	33	42	CAGTGCCCGCTGGAGAAGCTCTGGAGTCCGCCCGT	Q182@
2	GATC Biotech	Illumina HiSeq 2000, Unpaired 100 bp, 30-50 M reads	*10A005*	3							
2	GATC Biotech	Illumina HiSeq 2000, Unpaired 100 bp, 30-50 M reads	*10A008*	3L	*Notum*	*CG13076*	357G>A	39	46	GATCGTTCTACTCGAAGGTGGCTGGCACTGTTTCG	W119@
3	GATC Biotech	Illumina HiSeq 2000, Unpaired 100 bp, 30-50 M reads	*10A013*	3L	*ind*	*CG11551*	836C>T	69	56	CGGCGATTCTGGAACCAGATCTTCACCTGCTTCTCG	R279Q
3	GATC Biotech	Illumina HiSeq 2000, Unpaired 100 bp, 30-50 M reads	*10P009*	3							
4	GATC Biotech	Illumina HiSeq 2000, Unpaired 100 bp, 30-50 M reads	*11A017*	3R	*mira*	*CG12249*	1675G>A	39	54	GCTCCAGCGCTCCCTTGGCCAACTGCACCGATTCCA	Q559@
4	GATC Biotech	Illumina HiSeq 2000, Unpaired 100 bp, 30-50 M reads	*12A002*	3R	*Nup358*	*CG11856*	1669A>T	50	52	AAATTGCAAATCCAGCGTGAGGTGTATGACTCCTC	K557@
5	GATC Biotech	Illumina HiSeq 2000, Unpaired 100 bp, 30-50 M reads	*12A021*	3L	*ago*	*CG15010*	3272C>T	120	47	CCACTGACCACTCTGTTGAGAAATTCGTCAACAAT	G1091D
5	GATC Biotech	Illumina HiSeq 2000, Unpaired 100 bp, 30-50 M reads	*12C001*	3L	*sti*	*CG10522*	2881G>A	103	50	GCTCGGCCTTTTCCCATTGGCGGTGCTCCTTGAGGA	Q961@
6	GATC Biotech	Illumina HiSeq 2000, Unpaired 100 bp, 30-50 M reads	*12C004*	3R	*Surf6*	*CG4510*	112G>A	58	48	GATAGAACTTTTTGGTGATGGCGGGCAGGTCCTCC	Q38@
6	GATC Biotech	Illumina HiSeq 2000, Unpaired 100 bp, 30-50 M reads	*12C005*	3R	*lbe*	*CG6545*	85G>A	96	45	GCGTGGGCAGCGGGCTGGGGGCTCCGCCCACGGA	Q29@
7	GATC Biotech	Illumina HiSeq 2000, Unpaired 100 bp, 30-50 M reads	*12C011*	3R	*Scm*	*CG9495*	2404 G>A	24	50	GCGACCGCAGATGTGAGTTTGCCAAAGCAGAAGT	Q802@
7	GATC Biotech	Illumina HiSeq 2000, Unpaired 100 bp, 30-50 M reads	*12C042*	3L	*Pka-R1*	*CG42341*	124G>T	34	24	GCCACCACCCACCATCATCATCAGCATCAGCAGAA	A42S
							22A>T	31	19	ACGCTGGAGGAGCAGAGCCTGCGGGAGTGCGAA	T8S
8	GATC Biotech	Illumina HiSeq 2000, Unpaired 100 bp, 30-50 M reads	*01P030*	2R	*pea*	*CG8241*	2240C>T	50	60	CACAGTACTTCTTCAAGGCGCCAATCTTCACAATTC	S747L
8	GATC Biotech	Illumina HiSeq 2000, Unpaired 100 bp, 30-50 M reads	*03F047*	2R	*Prp8*	*CG8877*	4689C>T	64	47	CCAGAAAAGACCCTCCCACGTGGGGAAGTAGGTG	W1563@
9	GATC Biotech	Illumina HiSeq 2000, Unpaired 100 bp, 30-50 M reads	*03P028*	2R	*jhl-1*	*CG3298*	2125G>A	39	62	GCATATCCTCATCACTCGGTAATCGCGGGCACTTA	Q709@
9	GATC Biotech	Illumina HiSeq 2000, Unpaired 100 bp, 30-50 M reads	*03P016*	2							
10	GATC Biotech	Illumina HiSeq 2000, Unpaired 100 bp, 30-50 M reads	*05P009*	2L	*brat*	*CG10719*	940C>T	51	29	CAACAACAACAGCAGCAGCAACAGCAGCAGCGA	Q314@
10	GATC Biotech	Illumina HiSeq 2000, Unpaired 100 bp, 30-50 M reads	*03F083*	2L	*CycE*	*CG3938*	829G>A	49	47	GCTGGCTGCAGCCGGAGGAGGCTGGAGAAATTGT	Q277@
11	GeneWhiz	Illumina HiSeq 2000, Unpaired 50 bp, 50-80 M reads	*05P024*	2L	*CycE*	*CG3938*	1513G>A	29	62	GCGGGTAGATAAAGGCATCGTCCGCCTCCGCGCTC	Q505@
11	GeneWhiz	Illumina HiSeq 2000, Unpaired 50 bp, 50-80 M reads	*08P011*	3							
12	GeneWhiz	Illumina HiSeq 2000, Unpaired 50 bp, 50-80 M reads	*05P024*	2L	*CycE*	*CG3938*	see 11			see 11	see 11
12	GeneWhiz	Illumina HiSeq 2000, Unpaired 50 bp, 50-80 M reads	*13A023*	3L	*mop*	*CG9311*	2446G>A	34	44	GCTGTTGCTGCTGATACATGGGATTCGTGTAGCCG	Q816@
	PCR, Sanger Seq										
13	GATC Biotech		*08C065*	3	*Sce*	*CG5595*	1315C>T			CAGCAGTTGGTTATCCTGAATGGCAACCAGACGT	Q401>@